ABSTRACT

OCHI-OKORIE, CHIDIEBERE EBENEZER. Feasibility Analysis of Molecule Sensor for Detection and Quantification. (Under the direction of Dr. H. Troy Nagle).

The purpose of this investigation is to assess the feasibility of a molecule-sensor design for detecting and quantifying charge-neutral compounds in particular. Neutral molecules can be induced to translate by their exposure to a non-uniform electric field. Secondly, when a voltage is applied across saline electrolyte, the solution responds to vibration by generating a potential difference. The present molecule-sensor design is an attempt to combine these two phenomena whereby electric-field induced molecular vibration is detected by the energized electrolyte. In current experiments, the resulting sensor output deviated from theoretical expectations. Hence, the feasibility of this sensor arrangement is still in question. Areas for future investigation are proposed to further elucidate its properties.

Feasibility Analysis of Molecule Sensor for Detection and Quantification

by
Chidiebere Ebenezer Ochi-Okorie

A thesis submitted to the Graduate Faculty of
North Carolina State University
in partial fulfillment of the
requirements for the degree of
Master of Science

Electrical Engineering

Raleigh, North Carolina

2012

APPROVED BY:

_____	_____
Dr. H. Troy Nagle (*Chair*)	Dr. Gregory McCarty

_____

Dr. Ginger Yu

BIOGRAPHY

All people are ordinary. But some believe they can achieve the extraordinary, and so they try.

ACKNOWLEDGMENTS

Gratitude to the IXYS Corporation for freely supplying high-voltage transistors.

TABLE OF CONTENTS

LIST OF TABLES

LIST OF FIGURES

Introduction

The aim of this study was to examine the feasibility of a conceived chemical sensor. Such a device will serve the purpose of analyzing liquid samples to determine the presence and concentration of (charge-neutral) compounds in the samples. It is beyond the scope of this work to examine all the properties of such a sensor, as they are numerous and require further investigation.

The operation of the sensor is based on two experimentally observed phenomena. The first is a method for manipulating primarily neutral molecules by using electric fields, causing the molecules to move in response to the field. The second phenomenon is the observation that saline is sensitive to vibration when it conducts an electric current. Thus it was one hypothesis that both phenomena may be combined to create a molecular sensor comprising a method to induce motion of molecules and a method to detect this motion. Another hypothesis was that molecules of different types will have different mobility under the same conditions, and so may be distinguished.

Below, each of the two key phenomena is examined in turn. Then what follows is a description of a model in which these phenomena are applied in conjunction to implement a molecule sensor. Subsequently, experiments that test this model and its associated hypotheses are described.

First Phenomenon: Electric-Field Induced Neutral-Molecule Motion

Rotation of neutral molecules about their polar axis to align with an electric field is a basic concept in dielectric spectroscopy techniques. However, it may come as a surprise that neutral molecules will move (traverse a distance) under the influence of a suitable electric field, similar to the behavior of ions. This behavior was predicted from the observation that since neutral molecules rotate in a uniform electric field, it would make sense that they translate in a non-uniform field. This prediction comes by noting that rotation may be explained by equal and opposite forces acting on the positive and negative partial charges (dipole) of a neutral molecule. Thus, if these two forces were made unequal by applying a non-uniform field, the

neutral molecule would move in the direction where the electric field was strongest. This concept has empirical support. In a 2004 paper, Tsori et al reported the use of non-uniform electric fields to substantially separate neutral compounds of different types, where the cause of separation is explained in terms of molecule polarity [1]. A more polar compound displaces a less polar compound in the region of strongest electric field in a field gradient.

Figure 1 shows the design for a set of metallic rods and plate that will serve the purpose of generating a non-uniform electric field (e-field). We will use the term "plates" or "e-field generator" to collectively refer to the two rods and rectangular plate in figure 1. In the current design, the plates have a length of about 5 millimeters and rods A and C, which are spaced apart by ~2 millimeters, are both raised above plate B by 1 millimeter.

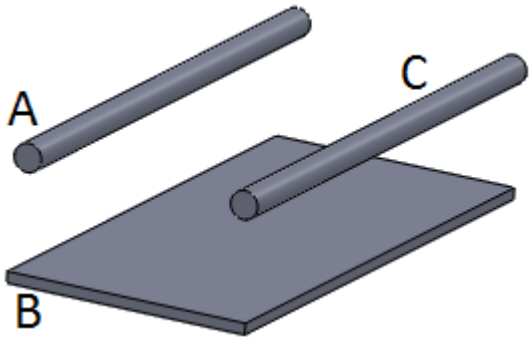

Fig 1 E-field generator consisting of three metal "plates," A, B, & C. The plates are ~5 [mm] long. Distance between plates A & C is ~2 [mm]. Plates A & C are raised ~1 [mm] above plate B.

Another perspective of the depiction in figure 1 appears in figure 2 with an addition: between the plates is a container that holds a mixture of electrolyte and at least one type of neutral compound to be detected. At any given time, the electric field produced by the e-field generator is activated in one of two states. The first state is what is shown in figure 2 and the second appears in figure 3. Switching back and forth between the two states moves neutral molecules that are contained within the field in a back and forth manner, as illustrated. An exemplary molecule is rendered in the figures as a white, stylized particle. The size of the molecule in the

figures is highly exaggerated. Provided below is further elaboration on the principles of operation of the e-field generator.

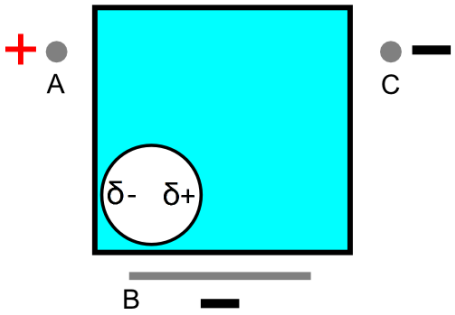

Fig 2 E-field generator consisting of three metal "plates," A, B, and C. Not drawn to scale. A sample container is positioned inside the generator. One of the plates is connected to the positive terminal of a voltage source and the other two plates are connected to the negative terminal of the voltage source. Configuring the connections this way results in one of two states of the non-uniform electric field.

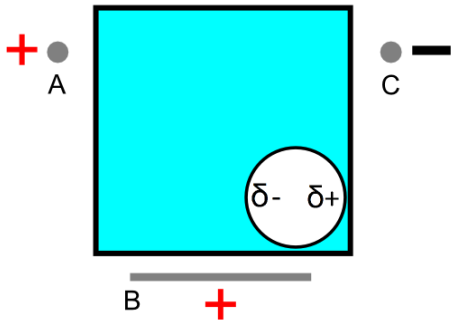

Fig 3 E-field generator as in figure 2, except with reversed polarity on plate B. This reversal results in the second of two states of the non-uniform electric-field. Not drawn to scale.

The neutral molecule depicted in figures 2 and 3 has partial charge separation (δ^+ and δ^-) or in other words, the molecule has a dipole. This dipole may be intrinsic or induced by the electric field. Continuing to examine figures 2 and 3, the rest of the sample solution is rendered in light

blue and the solution is enclosed by an insulator (black outline) so that electric-current flow is not possible from the plates into the solution.

A total of three plates comprise the e-field generator, of which two are rod-shaped and the third is planar. The plates are respectively labeled A, B, and C in figures 1-3. The charge-polarity on plates A and C are kept constant. That is, plate A remains positively charged and plate C remains negatively charged when the electric field changes state. On plate B, however, polarity is reversed between states. This reversal is in fact what creates the two e-field states. In the first state (figure 2), plate B is negatively charged. In the second state (figure 3), it is positively charged.

We now examine the two states of the electric field and their effects. In the first state, plate A has greater charge density than plate C. Therefore, the electric field in the vicinity of plate A is stronger than in the vicinity of plate C and the neutral analytes thereby migrate toward plate A, as shown in figure 2. For the second state in figure 3, analytes migrate in the other direction toward plate C where the electric is stronger. Simplified simulations of the electric for the first and second states respectively appear in figures 4 and 5.

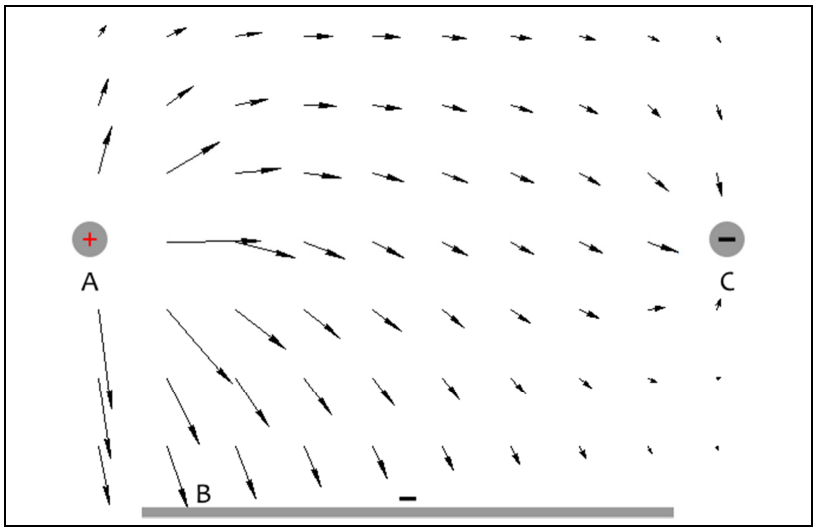

Fig 4 Simplified electric-field simulation to illustrate the first state of the e-field generator. As the vectors show, the electric field is strongest at plate A. Simulation was performed with QuickField™ electrostatics software.

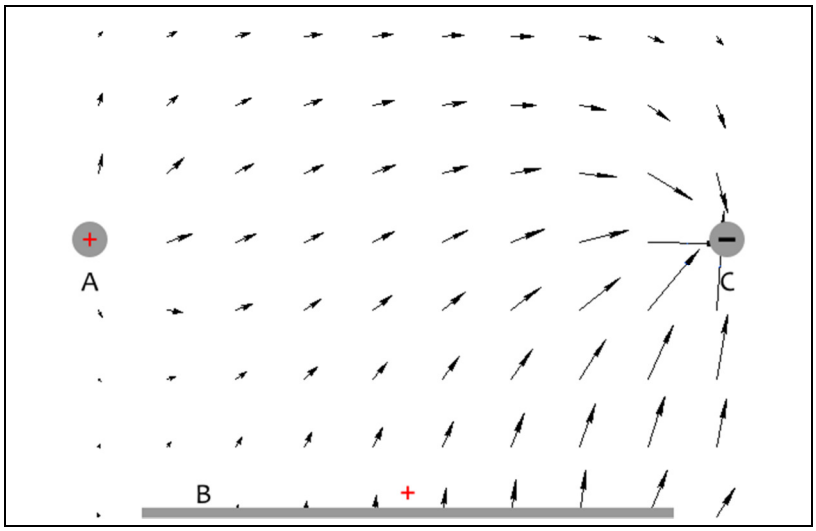

Fig 5 Simplified electric-field simulation to illustrate the second state of the e-field generator. As the vectors show, the electric field is strongest at plate C. Simulation was performed with QuickField™ electrostatics software.

Second Phenomenon: Motion-Sensitive Saline

The first phenomenon described above was a method to induce motion of neutral molecules by applying a non-uniform electric field. This section presents a second phenomenon: a motion-sensitive electrochemical device that may be useful for detecting molecular motion. A simple behavioral model for this device is provided based on both empirical observations and literature research. This model will describe only some of the properties of the system. Other unexplored properties of this motion-sensitive system are numerous and the objective of this study is not to examine them exhaustively, but to apply some of the known properties in order to assess the feasibility of a new molecular-sensor concept.

An example of a motion-sensitive device appears in figure 6, and is termed an *electrolyte-resistor voltage divider* (ERVD). The ERVD consists of a DC voltage source, an electrolyte solution (saline in this case) with two immersed electrodes, and a load resistor (R_L). The electrodes are made of copper or platinum in experiments presented below. The ERVD provides an output voltage (V_{out}), as labeled in figure 6. This output voltage varies with mechanical activity in the saline solution. Mechanical activity, that is, perturbation of the solution, temporarily changes the effective resistance of the solution, thus modulating the output voltage. The output voltage returns to its steady-state value when the disturbed solution is allowed to settle.

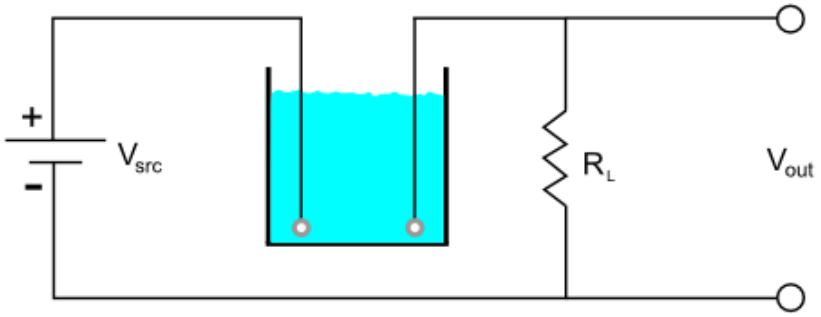

Fig 6 Electrolyte-resistor voltage divider (ERVD) consisting of voltage source, electrolyte solution (ex. saline), and a load resistor (R_L). V_{out} is the output voltage.

The following discussion is an exploration of empirical attributes of an ERVD. From these attributes, we develop a qualitative model for the system and then use this model to make a refined prediction of system response to stimulation.

Figure 7 presents an exemplary output-voltage profile for an ERVD at the moment it is powered on (when the voltage source is turned on). Output voltage jumps abruptly from zero to some high value when the input DC voltage source is turned on. Over time (several minutes, depending on configuration), this output voltage settles to an equilibrium value. Settling will occur more quickly if the input voltage from the DC source is initially set to a high value, then reduced to the operating value. Figure 8 shows the output voltage when the system has settled. This equilibrium output voltage remains stable for the duration over which it is observed (more than one hour).

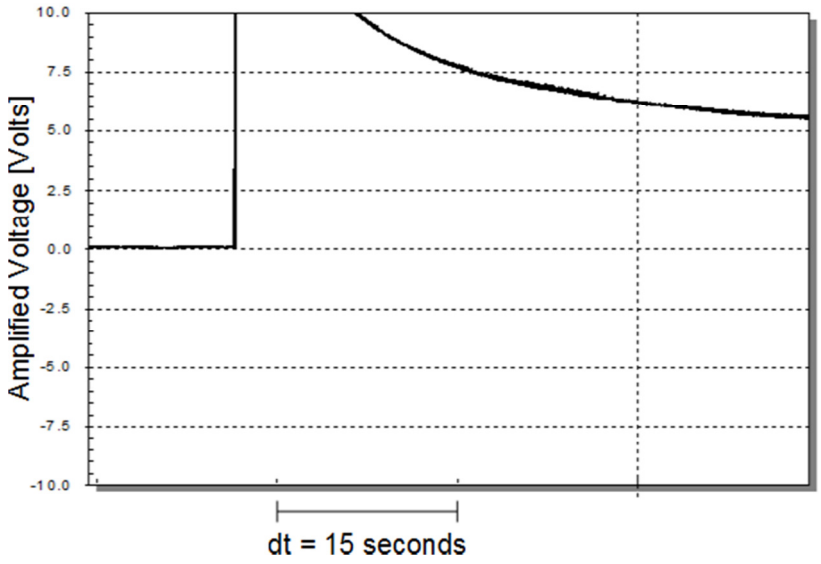

Fig 7 Start-up of ERVD showing ERVD output-voltage vs. time. Output-voltage is amplified 1000X. The ERVD voltage source (V_{src}) is set to 0.1 [V] and R_L is 1 [KΩ]. The electrolyte is saline and electrodes are made of copper. A 15-second interval is marked on the horizontal axis. Data acquisition rate is 100 [Hz].

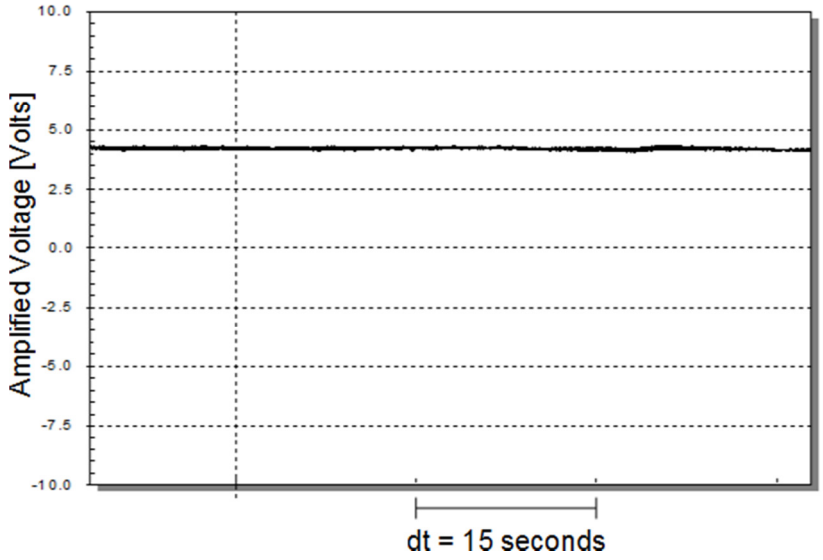

Fig 8 ERVD at equilibrium. Screenshot shows ERVD output-voltage vs. time. Output-voltage is amplified 1000X. The ERVD voltage source (V_{src}) is set to 0.1 [V] and R_L is 1 [KΩ]. The electrolyte is saline and electrodes are made of copper. A 15-second interval is marked on the horizontal axis. Data acquisition rate is 100 [Hz]. Output-voltage remained relatively stable for duration observed (more than 1 hour).

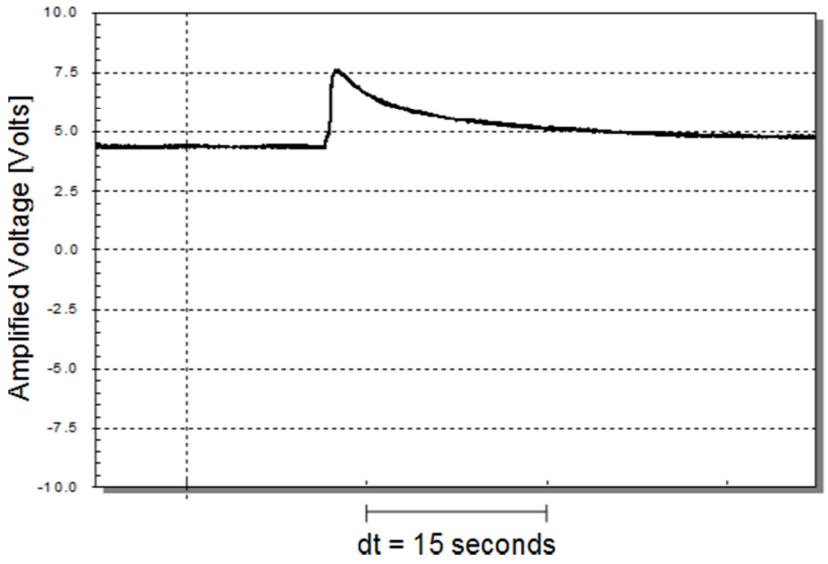

Fig 9 Perturbation of ERVD by stirring. Screenshot shows ERVD output-voltage vs. time with output-voltage amplified 1000X. The ERVD voltage source (V_{src}) is set to 0.1 [V] and R_L is 1 [KΩ]. The electrolyte is saline and electrodes are made of copper. A 15-second interval is marked on the horizontal axis. Data acquisition rate is 100 [Hz].

Figure 9 demonstrates what occurs when the saline solution is perturbed by vibrating the solution container or by stirring the solution, for example. The output voltage increases, then declines back to its equilibrium level as the solution comes to rest.

In light of the observations in figures 7-9 and based on fundamental concepts from electrophoresis, a simple model for the ERVD can be developed that is suitable for the purposes of this investigation.

To explain why the output voltage of an ERVD starts out and then settles to an equilibrium value following power up, we consider that the saline solution contains ions that migrate in response to voltage applied on the immersed electrodes. According to Wright [3, p. 276-277] and other electrochemistry literature, Na^+ and Cl^- are the main ions that flow in a saline solution when it is conducting electricity. In gel electrophoresis, a system that is similar in operation to a saline conductor, ions can be visually observed to move under the influence of an applied voltage, coming to a stop when they reach the electrode to which they have affinity. However, the experimental results in figure 8 demonstrate that not all ions in solution migrate to the electrodes. An appreciable current (~4 μA) continues to flow after the initial surge, indicating that ions remain in significant amounts throughout the solution.

Figures 7 and 8 thereby suggest that equilibrium is attained between the quantity of ions stationed at the electrodes and the quantity of ions in the rest of the solution. When the ERVD is initially powered, few ions are at the electrodes. Thus, ions begin to migrate to the electrodes, causing the output-voltage surge seen in figure 7. As ions accumulate at the electrodes, the concentration of ions at the electrodes hypothetically begins to approach a level that would not be sustainable; consequently, the flow of ions to the electrodes levels off, corresponding to the observed leveling of the ERVD output-voltage. Ion accumulation at the electrodes may be described by a charge double-layer model [5] where the negatively- or positively-charged electrode is complemented by ions of opposite charge from the electrolyte.

In figure 9, perturbing the solution appears to remove some of the accumulated ions at the electrodes (disruption of double-layer), thereby causing them to flow back to the electrodes. This return-flow generates additional current temporarily to restore the presumed charge double-layer, and thus the output-voltage rises and then falls.

From this model, we can predict that the motion-sensitive property of an ERVD is localized to its electrodes rather than the entire solution. This hypothesis was tested and the result appears in figure 10. When an electrode is stroked with a non-conducting rod, as if to brush off ions from the electrode, a sharp peak is observed. This stroking is performed twice to produce the result in figure 10. In contrast, stirring the entire solution in this experiment produces a similar result to that shown for the experiment in figure 9 – a broad peak is observed. These results are consistent with the model of electrode-localized sensitivity. Perturbation at the electrodes produces sharp, strong peaks; and perturbation away from the electrodes produces weaker, broader peaks. If the perturbation occurs far enough from the electrodes, then no response is observed.

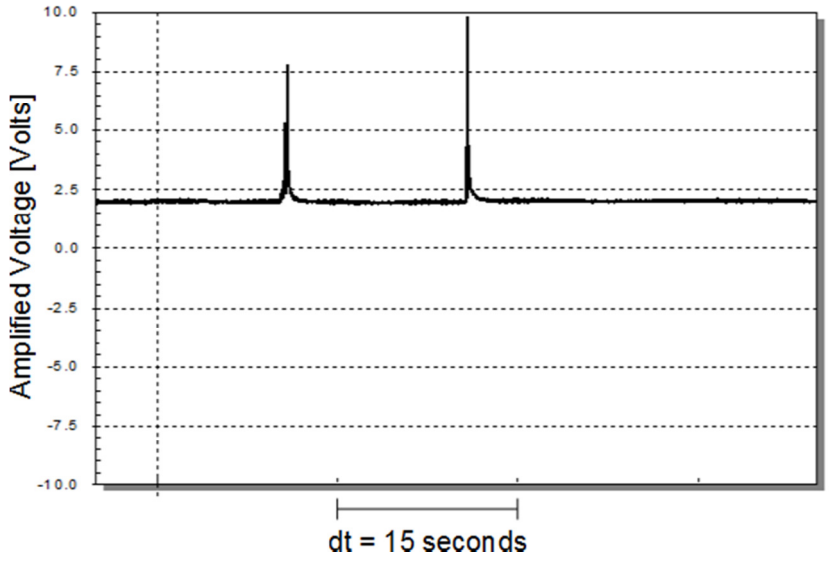

Fig 10 ERVD experiment similar to the experiment in figures 7-9. Screenshot shows ERVD output-voltage vs. time with output-voltage amplified 1000X. The ERVD voltage source (V_{src}) is set to 0.1 [V] and R_L is 1 [KΩ]. The electrolyte is saline and electrodes are made of copper. A 15-second interval is marked on the horizontal axis. Data acquisition rate is 100 [Hz]. One electrode of the ERVD is stroked twice with a non-conducting rod, producing a sharp peak for each stroke.

Combining the Two Phenomena

We have now described both a method to induce neutral-molecule motion and secondly a system that is sensitive to motion. The primary aim of this research work is to determine

whether these two phenomena can be combined effectively to create a sensor that will quantitatively detect and identify neutral molecules. The proposed approach for this combination is to prepare a mixture of electrolyte solution (ex. saline) that contains a small amount of neutral analytes. This mixture is then analyzed in what we may designate a "molecule motion sensor" (MMS), illustrated in figures 11 and 12. Below, we explore the hypothetical operation of the MMS.

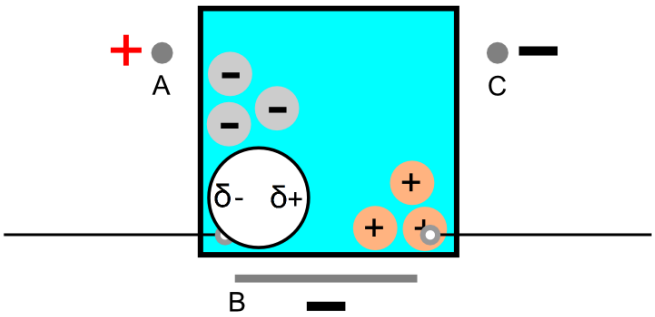

Fig 11 Molecule motion sensor (MMS), consisting of e-field generator and ERVD. The e-field is in the first of two states. Only the electrodes of the ERVD appear in the figure (load resistor and voltage source not shown). Not drawn to scale.

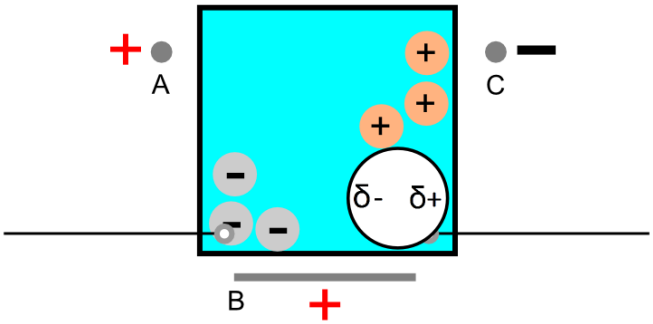

Fig 12 Molecule motion sensor (MMS), consisting of e-field generator and ERVD. The e-field is in the second of two states. Only the electrodes of the ERVD appear in the figure (load resistor and voltage source not shown). Not drawn to scale.

The MMS in figures 11 and 12 is comprised of an e-field generator and an ERVD. Not all components of the ERVD are illustrated in the figures. As shown, ions accumulate at the electrodes of the ERVD; and as described previously, the e-field generator creates a non-uniform electric field with two possible states. Switching back and forth between these states translates neutral molecules back and forth in the container. Figure 11 shows one state of the electric field. Figure 12 shows the second state. Ionic molecules, on the other hand, do not respond to the change in electric-field state in this simplified model. Ionic molecules ordinarily remain stationary because charge polarity does not change at certain regions of the container, for example in proximity to plates A and C. In other words, it is predicted that any free ion will migrate toward a region that has a fixed charge polarity that is opposite to that of the ion and it will remain there. However, the movement of neutral molecules in the container will tend to perturb ions at the electrode, displacing them temporarily, as illustrated. The output voltage of the ERVD would reflect this perturbation.

To further elaborate on the operation of the MMS, a schematic representation of the MMS is presented in figure 13. The MMS has five electrical connections. The “Plate A (+)” terminal connects plate A (ex. figure 12) to the positive node of a voltage source; the “Plate C (-)” terminal connects plate C to the negative node of the same voltage source; and the “Plate B (+/-)” terminal connects plate B to a signal that switches between the positive and negative nodes of the voltage source. This switching occurs at an adjustable frequency. Finally, the “electrode voltage (+)” and “electrode voltage (-)” terminals respectively connect the two electrodes of the ERVD with the rest of the ERVD circuit. The ERVD circuit and the e-field generator are connected to separate voltage sources, thereby preventing undesired interference.

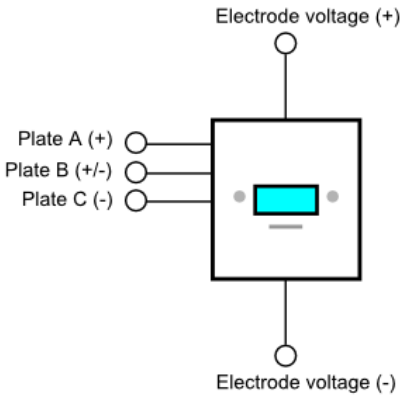

Fig 13 Schematic symbol for an MMS.

A pair of MMS devices may be employed for molecular analysis where one device contains the sample to be analyzed ("sample cell") and the other device serves as a reference ("reference cell"). This configuration appears in figure 14. The output voltage (v_{out}) for the pair is the difference between the output voltages of the individual devices. This reference configuration is chosen to mitigate artifacts that are not related to the nature of the analytes, and in essence cancels out noise signal.

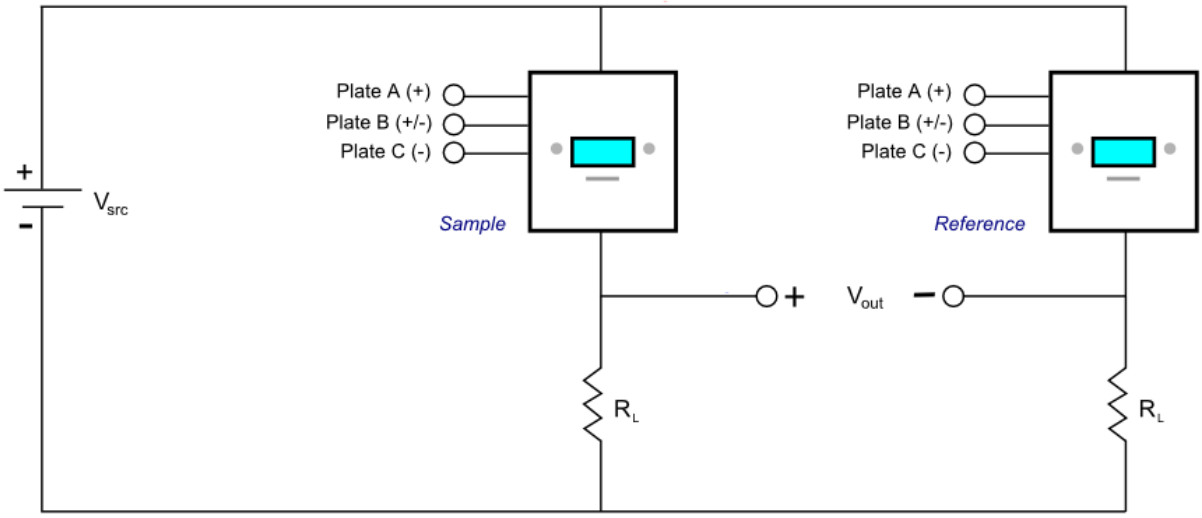

Fig 14 Schematic showing two MMS units employed in reference configuration.

Maximizing MMS Sensitivity

In this section, we explore potential approaches for maximizing the sensitivity of the MMS sensor pair in figure 14. Put another way, we will determine the conditions that will produce the largest output voltage when minimum amounts of chemical are analyzed in the MMS. To do so, we derive an expression for the output signal and inspect it for levers that can be adjusted to maximize sensitivity. In figure 14, the output voltage is given by

$$v_{out} = V_{src}\left(\frac{R_L}{R_L + r_s} - \frac{R_L}{R_L + r_r}\right), \quad (1)$$

where V_{src} is the voltage of the power source as shown, R_L is the value of the two identical load resistors, r_s is the effective resistance of the sample cell solution, and r_r is the effective resistance of the reference cell solution. Here, we have modeled the impedance of the electrolyte solutions as a variable resistor, similar to small-signal analysis of transistors at an operating point. For other applications, including scenarios where higher frequency signals are employed, more complex models may be useful [6].

When the sample and reference cells are at rest, v_{out} is ideally zero, resulting from the fact that r_s is ideally equal to r_r under this condition. When both cells are probed with the two-state electric field, the sample-cell electrodes will hypothetically be perturbed by the moving neutral analytes in solution, whereas the reference-cell solution remains at rest because it contains only electrolyte. As a result, r_s decreases whereas r_r does not change, thereby producing a positive output voltage. As apparent in equation 1, the magnitude of the output voltage may be boosted by using a larger value for V_{src}. This method is one possible way to increase the sensitivity of the MMS. In practice, V_{src} cannot be made arbitrarily large. In the types of experiments that have been conducted so far, V_{src} must be kept low enough to avoid currents in the milliamp range or higher. Such large currents result in vigorous bubbling (gas release) in the saline solution, creating undesired perturbation and altering the solution electrochemistry. This phenomenon may well be a result of exceeding the electrochemical window of the water solvent [7]. In the experimental setup employed below, the bubbling and sudden increase in current commences in the vicinity of 2.3 volts across the platinum electrodes.

A second lever for maximizing sensitivity is to optimize the value of R_L. Since R_L appears in both numerator and denominator of equation 1, predicting its effect on sensitivity is not as straightforward as in the case of V_{src}. We thereby proceed by exploring how the output signal, v_{out}, changes with R_L in order to find a value for R_L that will generate the largest output signal. Figure 15 is an exemplary plot of v_{out} vs. R_L when the sample cell is perturbed so that $r_s \neq r_r$. The values of r_s and r_r are fixed (held constant) in this simulated plot.

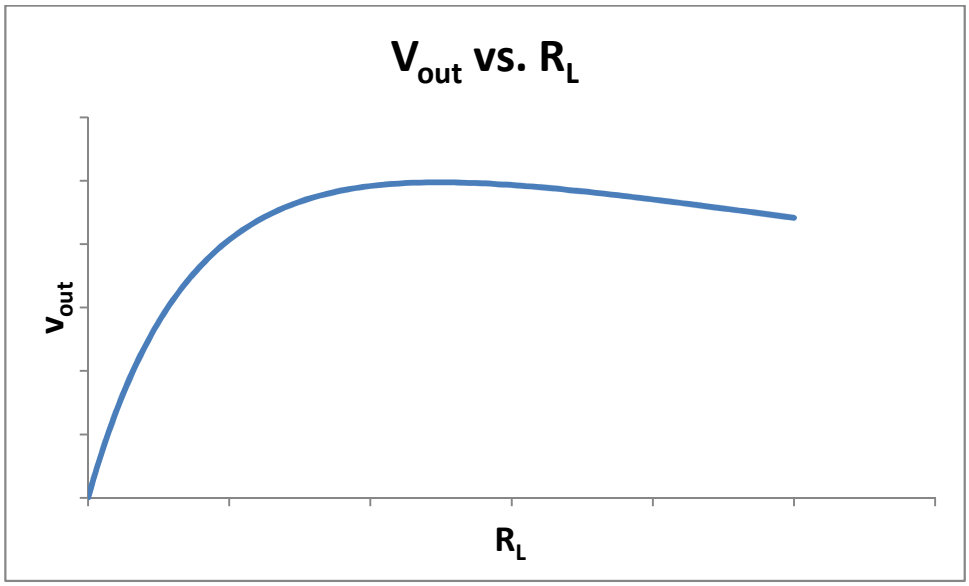

Fig 15 Exemplary simulated plot of v_{out} vs. R_L when $r_s \neq r_r$.

From the plot in figure 15, we see that the function v_{out} has a maximum. To calculate the value of R_L where this maximum occurs, we observe that the slope of the function v_{out} is zero at the maximum. Therefore, we can set the derivative (slope function) of v_{out} to zero and solve for R_L. The derivative of v_{out} with respect to R_L is

$$\frac{\partial}{\partial R_L} v_{out} = V_{src}\left[\frac{r_s}{(R_L+r_s)^2} - \frac{r_r}{(R_L+r_r)^2}\right]. \quad (2)$$

Setting this result to zero, we obtain

$$V_{src}\left[\frac{r_s}{(R_L+r_s)^2} - \frac{r_r}{(R_L+r_r)^2}\right] = 0. \quad (3)$$

Rearranging, we get

$$\frac{r_s}{(R_L+r_s)^2} = \frac{r_r}{(R_L+r_r)^2}. \quad (4)$$

Solving equation 4 for R_L, we obtain

$$R_L = \sqrt{r_s \cdot r_r}. \quad (5)$$

From equation 5, we can see that the optimal value for R_L is the geometric average of the sample-cell and reference-cell resistances. Though, r_r may be a fixed value, r_s changes when the sample solution is perturbed, resulting in a value of R_L that varies in equation 5. Since a fixed resistor will be used to implement R_L in the circuit, we wish to calculate a single optimum value for R_L. We do so by optimizing R_L for detecting weak perturbations, rather than any level of perturbation. While this new value of R_L may not be optimum for strong perturbations in the sample cell, it will be good enough because the detection threshold of the sensor has been minimized. To calculate this new value of R_L, we take the limit of R_L as r_s approaches r_r, the condition for weak perturbation:

$$\lim_{r_s \to r_r} R_L = \lim_{r_s \to r_r} \sqrt{r_s \cdot r_r} = r_r. \quad (6)$$

We conclude that the optimal value for R_L that will maximize the output signal is r_r when there is only weak perturbation. In other words, we adjust the value of R_L in the circuit until half the supply voltage falls across the R_L resistors ($R_L = r_r = r_s$ at equilibrium). Intuitively, it makes sense that the function v_{out} will have its maximum at $R_L = r_r$: examining equation 1, if R_L is too small or approaching zero ($R_L << r_r$), then the output will also approach zero. If on the other hand R_L is too large ($R_L >> r_r$), then the output will again go to zero. Thus, the maximum for v_{out} will occur at a non-extreme value of R_L.

Analysis Concepts

We now examine concepts that underlie the process of identifying and quantifying molecules in a sample using an MMS as the analysis tool. These concepts are: the relative quantity of analytes in the electrolyte solution of an MMS and the attenuation of molecular swing at high frequencies. After describing these concepts, we will proceed to demonstrate how they come into play in detecting molecules and measuring their concentration.

Relative Quantity of Analytes in Electrolyte Solution

Referring to figure 14, the sample cell of an MMS contains a mixture of electrolyte solution and neutral compounds ("analytes" or "sample"). The reference cell contains only electrolyte solution. Therefore the output signal of the MMS ideally represents the difference in composition between the two cells. In order to minimize secondary effects such as changes to the conductivity of the electrolyte solution, the relative quantity of analytes in the sample cell is kept small, for example 1% or less. Using small quantities of sample may prevent significant variation in the properties of the electrolyte solution from one experiment to the next when different types of samples are analyzed. Additionally, small quantities of sample minimize intermolecular interactions between analyte molecules so that each molecule behaves independently of others at various concentrations. This independence promotes a linear correspondence of analyte concentration with output signal.

Attenuation of Molecular Swing at High Frequencies

As shown in Figures 11 and 12, an electrode is positioned at each end of the container. If the electrodes are made of platinum, one is far more sensitive than the other. The sensitive electrode generates a significant positive voltage at the output when perturbed; whereas the relatively insensitive electrode slightly reduces the output voltage when there is a disturbance (negative contribution to the output). Neutral molecules translate from one end of the container to the opposite end when the electric-field changes state, thereby perturbing the solution. This back and forth change in state occurs at an adjustable frequency. At low frequency, perturbation is not significant and therefore there is little output. At mid-range frequency, a large positive output signal is detected. If the frequency is high enough, the molecules will not have sufficient time to migrate, or swing, across the container to reach the sensitive electrode, assuming the

migration is initiated at the other electrode. As frequency continues to increase, the distance traversed by the molecules per cycle will also decrease. This reduction in swing will hypothetically result in diminished perturbation of ions at the sensitive ERVD electrode; thus, output voltage falls. Figure 16 illustrates a hypothetical frequency sweep of the MMS sensor.

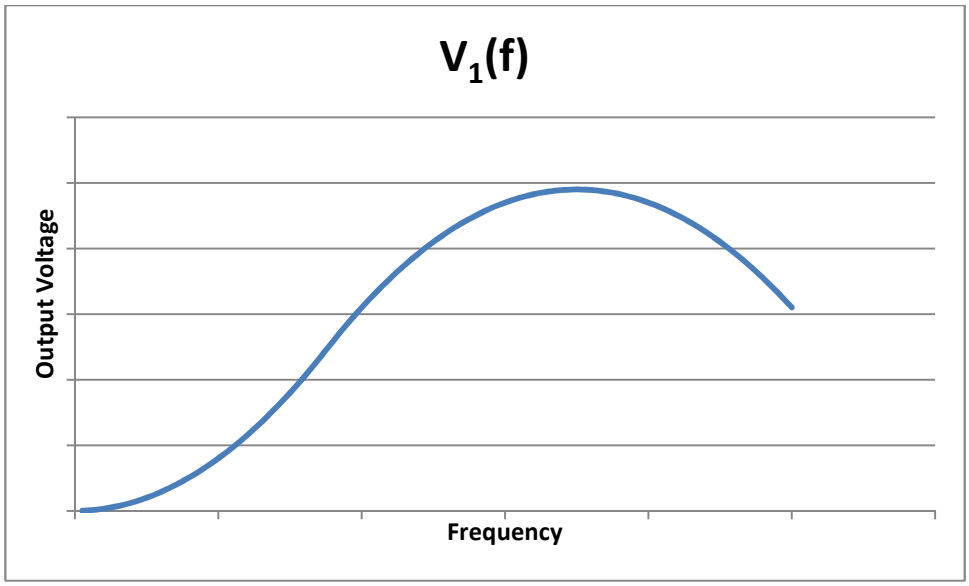

Fig 16 Hypothetical result of frequency sweep in an MMS pair comprised of a sample and a reference cell.

Referring to figure 16, frequency is swept from low to high value rather than from high to low value. This approach eliminates the settling time that would otherwise be required for the electrolyte solution if transitioning from higher to lower frequencies.

In figure 16, the sensor output reaches a maximum then begins to decrease. The range of frequencies where the output reverses direction and begins to decrease may be described as an "attenuation range." Assuming that the analyzed sample in figure 16 contains only one type of molecule, then the observed attenuation range may be characteristic of that compound. That is, different types of molecules may attenuate at unique frequency ranges. Figure 17 provides hypothetical examples of spectra for two different types of molecules ("molecule 1" and

"molecule 2"). Each of the two spectra attenuates at a different set of frequencies: $V_2(f)$, the spectrum of molecule 2, begins to decline when the output for molecule 1, $V_1(f)$, is still increasing.

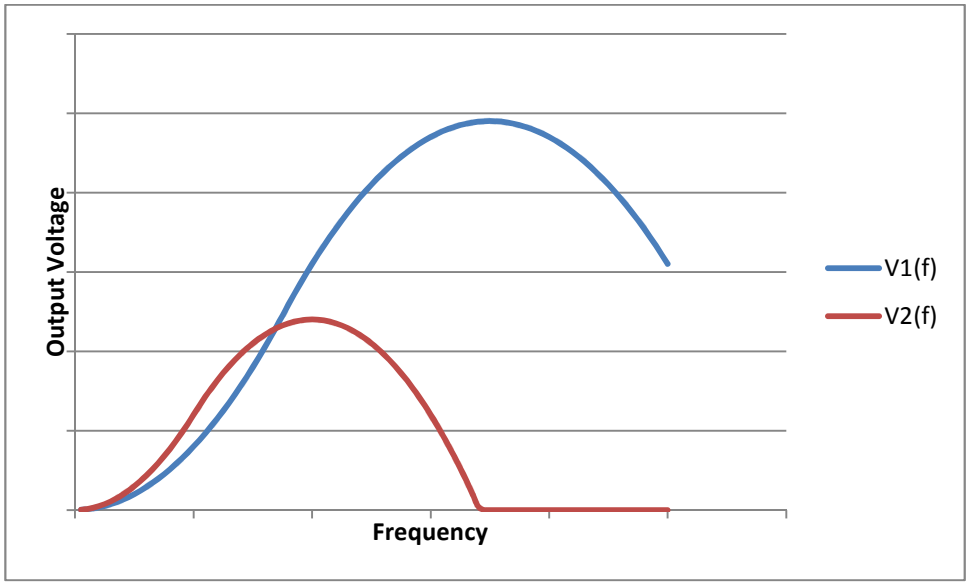

Fig 17 Two conceptual output signals, $V_1(f)$ and $V_2(f)$. $V_2(f)$ initially has a greater magnitude than $V_1(f)$ but attenuates earlier than $V_1(f)$.

The attenuation range of a molecule is presumed to be related to its ability to quickly respond to the state-switching electric field. Molecules that can move quickly will resist attenuation, resulting in an output that only declines at high frequencies. Slow-moving molecules are not able to respond as quickly to the state change and therefore may not traverse the extent of the container to reach the sensitive electrode. They therefore attenuate early at low frequencies. The agility of a molecule in the electric field depends on its properties including mass, shape, dielectric constant or dipole magnitude, and extent of intermolecular interaction with the surrounding medium (drag). Heavy and wide molecules with a weak dipole will tend to move slowly, whereas small molecules with a strong dipole would move quickly.

Standard Sample Approach

Based on the concepts described above, what we expect in the MMS is a sensor whose output is linear with respect to concentration (not illustrated) but has a nonlinear frequency response (ex. figure 16). Presented in this section is a method to extrapolate molecule concentration and identity by processing raw signals such as those modeled in figures 16 and 17. This method would be particularly useful in the situation where the sample to be analyzed contains more than one type of chemical, resulting in a complex raw signal in which a distinct signature for each molecule is difficult to ascertain. We may refer to this method as the "standard sample approach" (SSA).

The essence of the SSA is to employ the spectrum of a known chemical(s) at a known concentration to decipher the spectrum of an unknown sample. The known chemical serves as a comparative standard and hence is the "standard sample." Suppose the spectrum of the known sample is given by the function K(f) and that of the unknown sample is given by U(f). We may determine the identity and concentration of molecules in the unknown sample by deriving a quotient function Q(f) given by

$$Q(f) = \frac{U(f)}{K(f)}. \tag{7}$$

Essentially, we have divided the spectrum of the unknown sample point for point by the spectrum of the known sample. If for example, Q(f) = 1 at all frequencies, this result would indicate that the known and unknown samples are probably identical: they contain the same chemical(s) at the same concentration(s). In another example, if Q(f) = 0.8 across all frequencies, we can conclude that both samples are proportionally composed of the same chemical(s), but the concentration of the unknown sample is 80% that of the known sample. Figures 16 and 18 aid in illustrating this concept. $V_1(f)$ appears in figure 16 and in figure 18, K(f) = $V_1(f)$ and U(f) = $0.8 \cdot V_1(f)$.

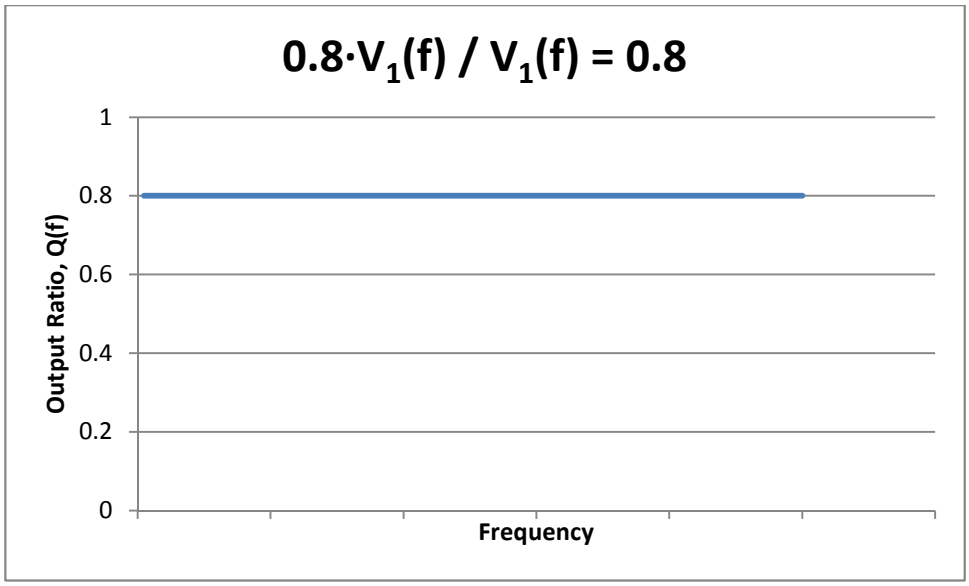

Fig 18 A linear quotient function resulting from comparison of chemically similar samples. The unknown and known samples differ only in analyte concentration.

In general, a test sample that proportionally contains the same chemicals as the standard sample but at a different concentration may have a spectrum U(f) given by

$$U(f) = c \cdot K(f), \tag{8}$$

where c is the concentration of the test sample relative to the standard sample. In this case, Q(f) = c. The absolute concentration of the test sample in terms of a specific unit may be obtained by multiplying c by some conversion factor α, where α is a constant.

In another scenario where the standard sample and unknown sample have dissimilar chemical constituents, suppose that K(f) is equal to $V_1(f)$ in figure 16 and U(f) = $V_2(f)$ in the same figure. Assume $V_1(f)$ and $V_2(f)$ are spectra for two different types of molecules, molecule 1 and molecule 2. The two compounds have different attenuation ranges. The quotient function is given by

$$Q(f) = \frac{U(f)}{K(f)} = \frac{V_2(f)}{V_1(f)}. \tag{9}$$

A plot of Q(f) appears in figure 19 below.

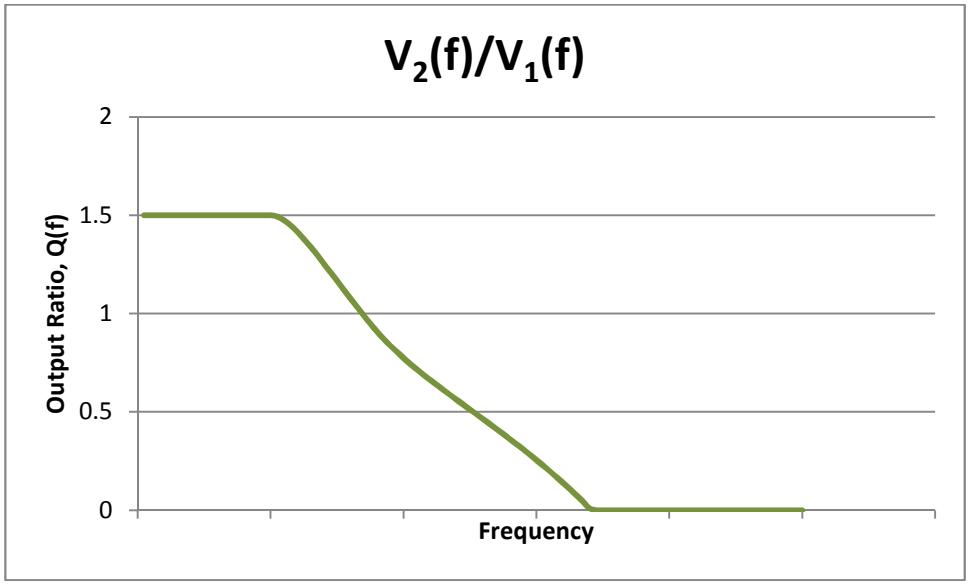

Fig 19 Quotient function resulting from comparison of chemically dissimilar samples. The unknown sample attenuates earlier than the standard sample.

As the plot of Q(f) in figure 19 is not a straight line, we can conclude that the standard sample is chemically dissimilar to the unknown sample. The relative concentration of the unknown sample (molecule 2) can still be obtained. Molecule 2 attenuates before molecule 1, hence the quotient function declines in value. We can obtain the relative concentration of molecule 2 before this decline occurs by taking the value of Q(f) at a low frequency. In the case of figure 19, c = 1.5. The absolute concentration of molecule 2 may be expressed as $\beta \cdot c$, where β is a constant that depends both on the unit of concentration employed and on the behavior of molecule 2 in the sensor. The identity of molecule 2 may be determined by observing its attenuation pattern and frequency range in Q(f).

Figure 20 presents another scenario. Here, the quotient function is similar to that in figure 19, except that it has a higher initial value and attenuates to a value of 1, instead of 0 as in figure 19.

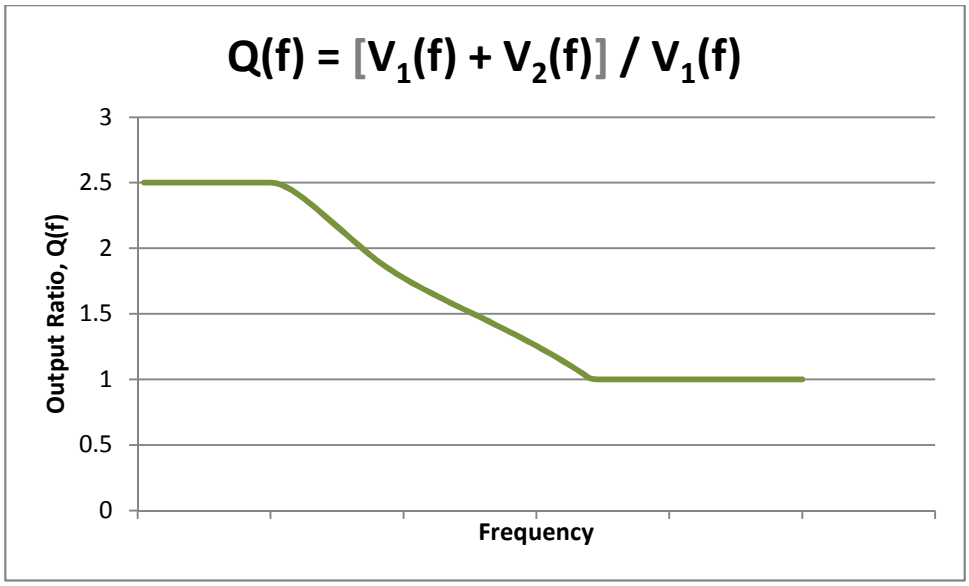

Fig 20 Varying quotient function resulting from comparison of a solution containing two types of molecules and a solution containing only one of the compounds.

We may interpret Q(f) in figure 20 to represent a sample that is a mixture of molecule 1 and molecule 2. At low frequencies, both compounds contribute to the output. At higher frequencies, molecule 2 attenuates and no longer contributes to the output. In this case,

$$Q(f) = \left[\frac{V_1(f) + V_2(f)}{V_1(f)}\right] = 1 + \frac{V_2(f)}{V_1(f)}. \quad (10)$$

When $V_2(f)$ diminishes to zero, Q(f) = 1, as figure 20 illustrates. The relative concentration of molecule 1 is calculated by taking the value of Q(f) after attenuation of molecule 2; in this case, Q(f) = 1. Similarly, the relative concentration of molecule 2 may be calculated by subtracting the concentration of molecule 1 from the total concentration: 2.5 – 1 = 1.5. Thus, the relative concentration of molecule 2 is 1.5. The same technique may be applied to analyze any unknown sample with spectrum U(f), provided that each type of molecule in the sample has a distinct attenuation range. Where attenuation ranges overlap, other techniques such as observing changes in slope and the frequencies where the changes occur may be employed to both identify the molecules and determine their concentration. Figure 21 is a plot of a quotient function for a hypothetical sample that contains three analytes in addition to a standard sample.

Attenuation ranges for each type of molecule is marked in the figure, with molecule types 1 and 2 having overlapping ranges in part of the spectrum.

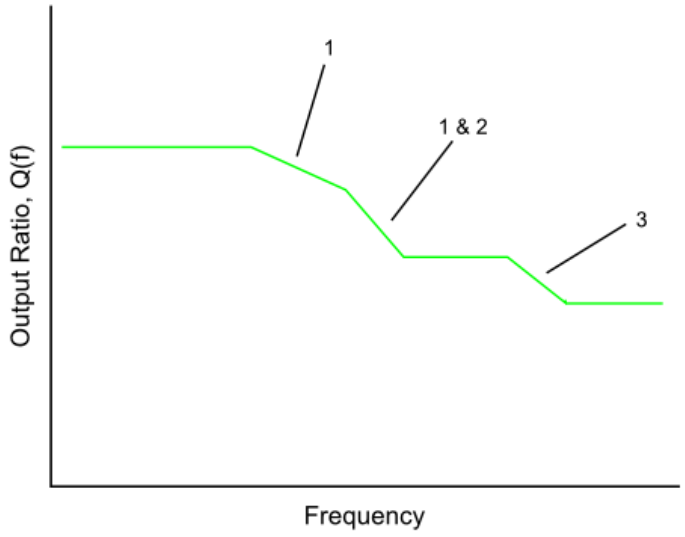

Fig 21 Quotient function where unknown sample contains three types of analytes in addition to chemical(s) in the standard sample.

Nested Sweeps of Electric Field and Frequency to Discover Attenuation Ranges

The strength of the electric field between the plates of the e-field generator has a direct impact on the speed of analytes as they migrate from one wall of the solution container to the opposite wall. If molecules are moving so quickly that attenuation is not observed within the frequency arrange available for a sweep, the electric-field strength may be lowered in order to slow down the molecules. A systematic approach for discovering attenuation ranges of analytes would be to perform nested sweeps: the electric-field strength is set to an initial level and then a frequency sweep is performed. The electric-field strength is then increased and another frequency sweep is performed. This process may be repeated as necessary. Fast-moving molecules would hypothetically be detected at low field strengths whereas under the same conditions, slow-moving molecules will produce weak signals and may not be detected. In contrast, at high field strength, fast moving molecules will not attenuate, whereas slow-moving

molecules will exhibit detectable swing attenuation. For a given analyte, each step increase in the electric-field strength may produce at most one attenuation range.

Experiments

This section presents experimental results from testing the above hypotheses. We proceed by briefly describing the methods of the experiments and then follow with results. In the next section, we discuss conclusions drawn from the results.

In each experiment, a sample containing analyte is placed in the sample cell of an MMS pair; and a sample containing only saline is placed in the reference cell. The analyte in the sample cell constitutes 1% of the sample solution by mass. This sample solution is prepared by mixing 0.1 [g] of analyte with 9.9 [g] of saline solution. The stock saline is prepared by adding distilled water to 50 [g] of salt (NaCl) for a total solution volume of 250 [mL]. Experiments are conducted at room temperature. R_L for both sample and reference cells is set to 250 [KΩ]. V_{src} is set to 4.15 [V] so that r_s and r_r, which vary with V_{src}, are ≅ 250 [KΩ] at equilibrium. The voltage between Plate A and Plate C is 2400 [V]; and Plate B switches between 2400 [V] and 0 [V], thereby creating the time-varying electric field. The switching frequency of the field starts at 100 [Hz] and increments by 100 [Hz] for the next data point, with the frequency sweep ending at 5 [KHz]. In the plots, Δv_{out} ("delta v_{out}") on the y-axis is the change in v_{out} rather the actual value of v_{out}.

Figure 22 is a photo of the sample and reference cells, which are separated by an impermeable wall. The cells are made of WaterShed XC 11122 material and manufactured by FineLine Prototyping, Inc using 0.002" resolution stereolithography. Both cells are recessed at the bottom. The sensing electrodes are housed in these 1 [mm]-deep recesses and are 99.95% platinum metal. Appendix E covers cell configuration.

In experiments, both cells are filled with 1 [mL] of solution and then the ERVD circuit is powered on. After approximately 1 minute of settling, 700 [μL] of solution is removed from each cell and a lid is placed over the recess in the cells. The lid is made of the same material as the cells. Once the sensor output settles again, data acquisition commences. From empirical observation, starting with a larger sample volume than is required for analysis increases

detector sensitivity several fold, possibly by increasing ion accumulation at the electrodes. The excess volume is then removed prior to data acquisition. Removal of this excess volume after settling does not noticeably alter sensitivity.

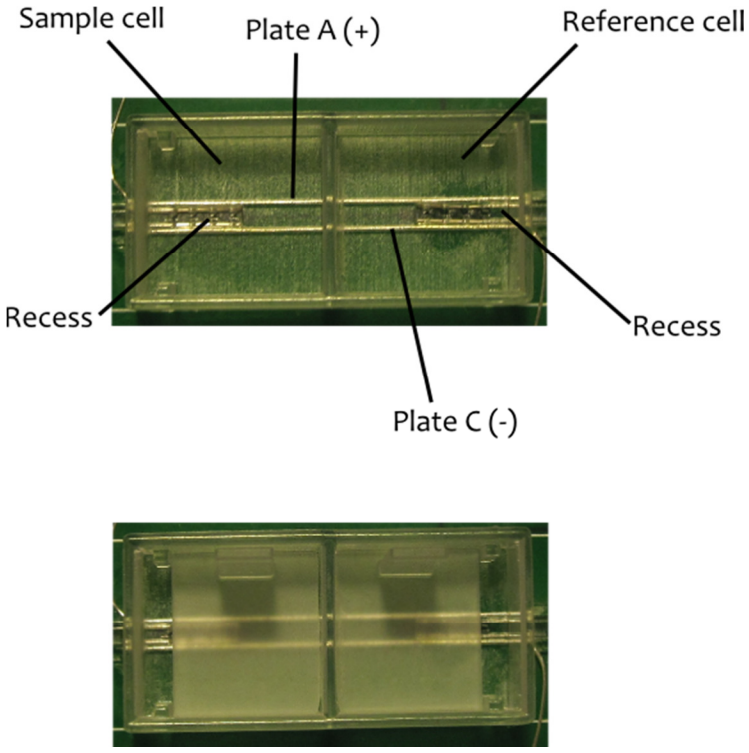

Fig 22 Receptacle comprised of sample and reference cells. In the lower image, the recesses in both cells covered with lids. A 0.5 [mm] by 0.5 [mm] section of each recess is not covered by the lids in order to allow released gases to vent. Recesses are 1 [mm] deep. The electrodes in the recesses come in contact with the solution. Plates A and C are insulated and do not make contact with the solution. Plate B is positioned beneath the recesses and is not visible in the images.

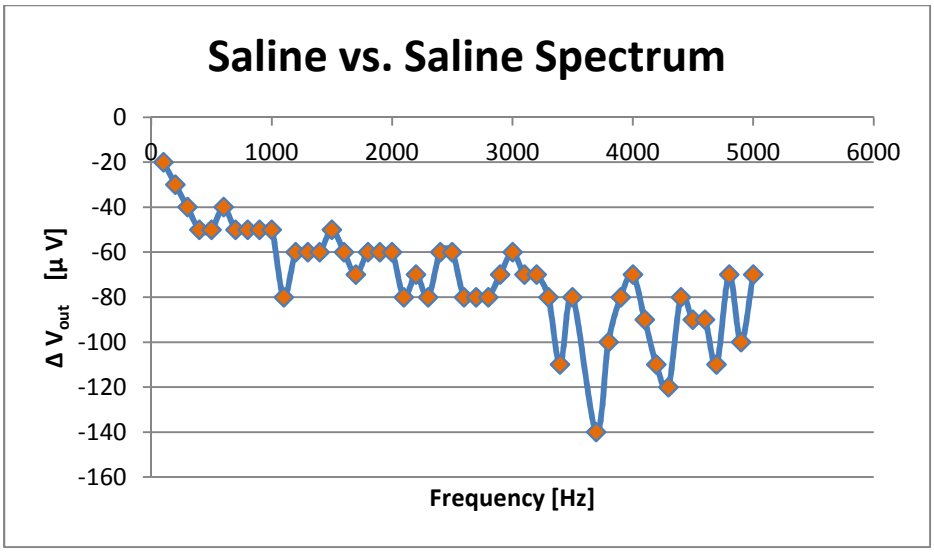

Fig 23 Saline vs. Saline spectrum. Both the sample and the reference cells of the sensor contain only saline solution in this control experiment. The point sampled at frequency 3600 [Hz] is not shown in the plot as it is an extreme, random outlier most likely caused by generated bubbles that burst.

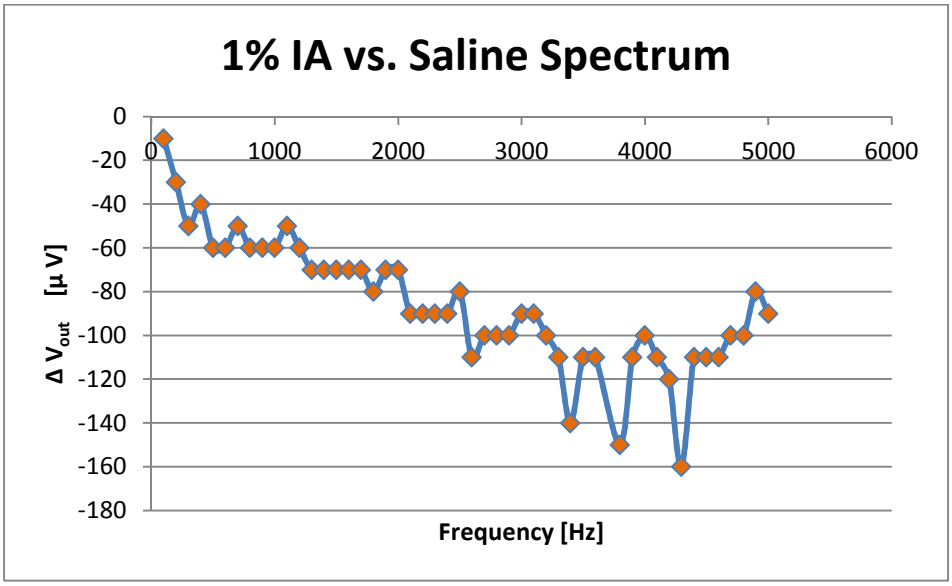

Fig 24 1% Isopropyl Alcohol (IA) vs. Saline Spectrum. Data from analysis of 1% isopropyl alcohol in the sample cell and saline in the reference cell. The point sampled at frequency 3700 [Hz] is not shown in the plot as it is an extreme, random outlier most likely caused by a generated bubble that burst.

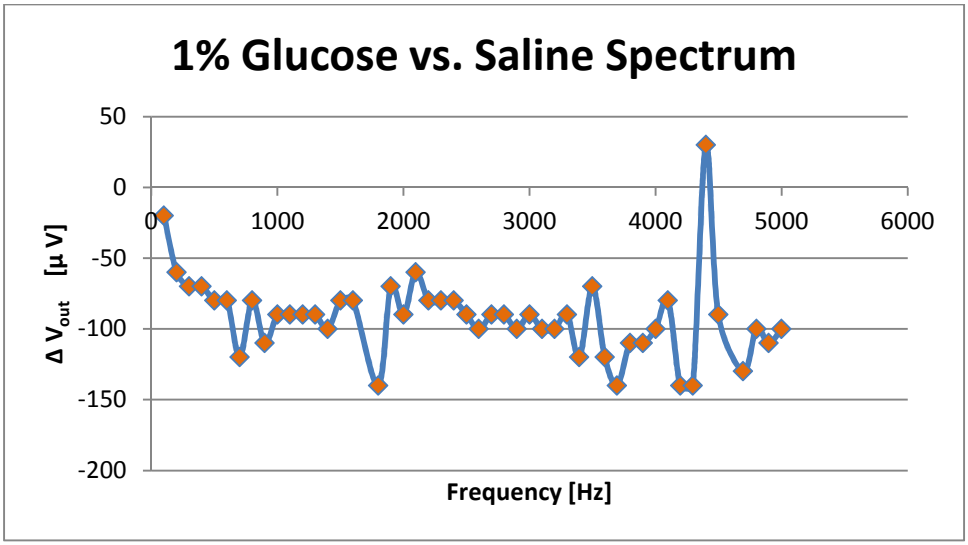

Fig 25 1% Glucose vs. Saline Spectrum. Data from analysis of 1% glucose in the sample cell and saline in the reference cell. The points sampled at frequencies 1700 [Hz] and 4600 [Hz] are not shown in the plot as they are extreme, random outliers most likely caused by generated bubbles that burst.

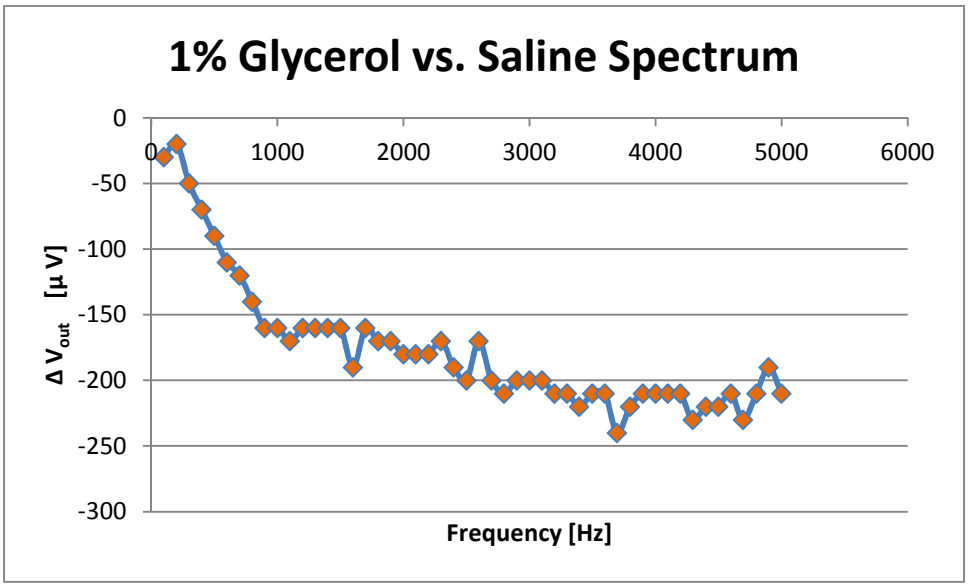

Fig 26 1% Glycerol vs. Saline Spectrum. Data from analysis of 1% glycerol in the sample cell and saline in the reference cell.

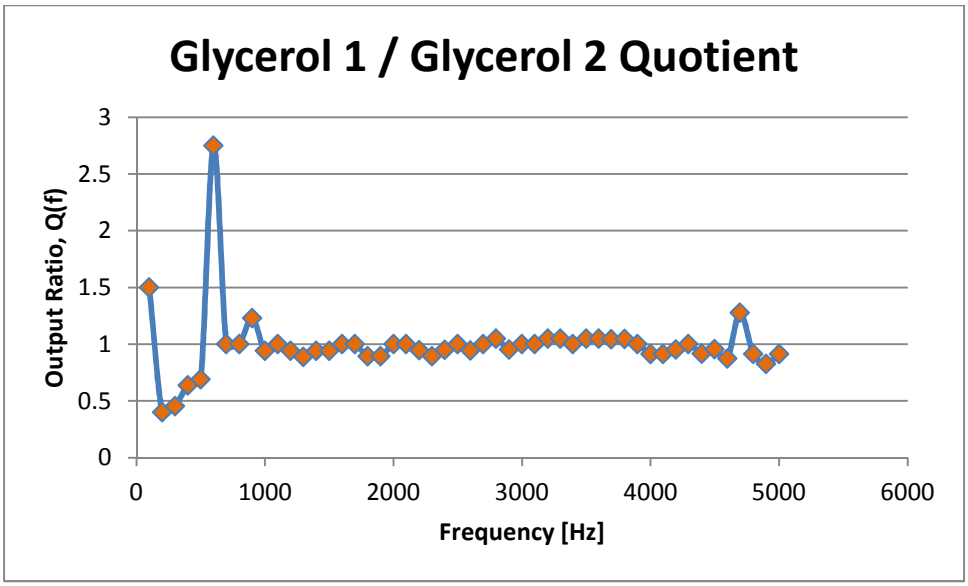

Fig 27 Quotient function of two spectra of 1% glycerol vs. saline. The sample cell contains 1% glycerol and the reference cell contains saline. The same sample set is analyzed twice in the sensor in order to perform a sensor consistency check.

Discussion

In some of the data presented, one or two data points were not included in the plot as they are outliers. These outliers are not considered relevant because they are most likely caused by bubbles that burst in the sample or reference cell, resulting in undesired perturbation. The bubbles arise from gases that form at the electrodes.

Perhaps the most pertinent observation in reviewing the data in figures 23-26 above is that the change in output voltage (delta v_{out}) is negative rather than positive. This result squarely contradicts expectations and suggests a systematic artifact. As the sample cell of the sensor contains analyte and the reference cell does not, we would expect a positive output voltage. Further scrutiny of the sensor performance and additional experimentation is required to either confirm or invalidate the above results.

In much of the data (except the glucose analysis), the output follows a trend of becoming increasingly more negative. However, as this trend also holds in the control experiment of

figure 23, it is more than likely only an artifact as opposed to related to the nature of the analytes. The contents of the sample and reference cells are identical in the control experiment: they both hold saline only.

In light of the unexpected results, it was important to determine at the minimum whether the sensor readings were consistent. One approach was to analyze a particular sample twice and compare the data from both readings point by point. The plot in figure 27 above is an example of this comparison: we obtain the quotient function for two spectra from a 1% glycerol vs. saline experiment. We would expect this quotient function to have a value of 1 across all frequencies. We nearly obtain this result in figure 27. This outcome largely holds for other experiments. We can thus conclude that despite the negative output of the sensor, it performs fairly consistently.

If the relatively weak artifact-signals are ignored, then in effect the sensor has zero output; that is, the applied electric field does not induce detectable molecule motion. This result may stem from a number of factors. One important factor is the electric-field strength. The applied transient electric field may not be sufficiently strong to induce molecular motion, considering the types of compounds that were assayed. Past experiments leading up to this study and those by Tsori et al [1], have either exclusively analyzed nonpolar molecules or a combination of nonpolar and polar molecules. In contrast, the experiments presented here exclusively analyze polar molecules (water, glucose, glycerol, isopropyl alcohol). As a result of their polar nature, these compounds are expected to less readily separate under the influence of an electric field.

A lack of significant output signal from the sensor precludes analysis of attenuation ranges or determination of concentration. In summary, the detector function (ERVD) of the sensor is operational; however, the effectiveness of the e-field perturbation scheme requires further investigation.

Future Studies

One experimental approach to scrutinize the above results while minimizing the possibility of artifacts is to design a simpler prototype where the electric field pattern is altered mechanically, rather than by electrical switching. This approach will make it possible to create much stronger

electric fields without generating potentially interfering signals. The objective of this simplified experiment would only be to determine whether a transient electric field has an unmistakable impact on an ERVD output. More elaborate experiments can follow if the result is positive.

A large number of factors come into play in the MMS. For example, a variety of electrolytes may be employed in an MMS and may each produce unique results to allow unambiguous identification of more compounds. The mechanism of current flow in select electrolyte solutions may be examined further. The size and shape of the ERVD electrodes possibly are important variables that affect ion accumulation and thus sensitivity. It may also be useful to determine various analytical relationships, for example, the effect of electric-field strength on the attenuation range of an analyte and the impact of changes in temperature. Miniaturization of the MMS system from millimeter to micrometer scale is another consideration. These factors may be explored in future studies. Improved methods for precisely perturbing the ERVD electrolyte would prove useful in such studies.

REFERENCES

[1] Tsori Y, Tournilhac F, Leibler L. Demixing in Simple Fluids Induced by Electric Field Gradients. Nature 2004; 430: 544-547

[2] Tsori Y, Leibler L. Phase-Separation in Ion-Containing Mixtures in Electric Fields. PNAS 2007; 104 (18): 7348-7350

[3] Wright, Margaret Robson. 2007. An Introduction to Aqueous Electrolyte Solutions. John Wiley & Sons Ltd, England.

[4] Kremer F, Schönhals A. 2003. Broadband Dielectric Spectroscopy. Springer-Verlag, Berlin, Germany.

[5] Koryta J, Dvorak J, and Kavan L. 1993. Principles of Electrochemistry. 2nd ed. p. 198-244. Wiley Publishers, Chichester, England.

[6] Webster J. 1997. Medical Instrumentation: Application and Design. 3rd ed. p. 183-200. John Wiley & Sons Ltd, Hoboken, New Jersey.

[7] Bockris J, and Reddy A. 1998. Modern Electrochemistry I: Ionics. 2nd ed. p. 720. Plenum Press, New York.

APPENDICES

APPENDIX A – System Design Overview

The electronics for the molecule-sensor prototype consist of a computer (PC), a data acquisition device (DAQ) controlled by software on the PC, and a custom-designed circuit (CC). The data acquisition device is a LabJack U3 (labjack.com). Descriptions of the main functions of each component are in table 1 below.

Table 1 Overview of Molecule-Sensor System Design

PC	DAQ	Custom Circuit (CC)
• Determine next switching frequency in frequency sweep • Signal DAQ to generate digital clock signal for selected frequency • Send signal to tare CC output, if necessary • Sample data point at the new frequency • Repeat above at next frequency	• Handle communication between PC and CC (AD and DA conversions) • Generate square-wave switching signal (clock) at frequency specified by PC • Generate analog offset voltages for CC amplifier circuit	• Use clock signal from DAQ to switch electric-field across sample • Power ERVD • Amplify signal from sensing electrodes • Filter high frequency noise • Pass signal to DAQ for AD conversion • Isolate signals from high voltage

APPENDIX B – Circuit Schematics

Schematics for the sensor custom circuit (CC) appear below. The circuit has two main divisions. One division mediates generation of the state-switching electric field and the second division detects and amplifies output signal from the ERVD pair. The two divisions are electrically isolated to minimize interference. Additional data for selected components appear in Appendix C.

Figures 28-30 show overlapping snapshots of the first division of the circuit. The following is a description of this division of the circuit and the functions of its key components.

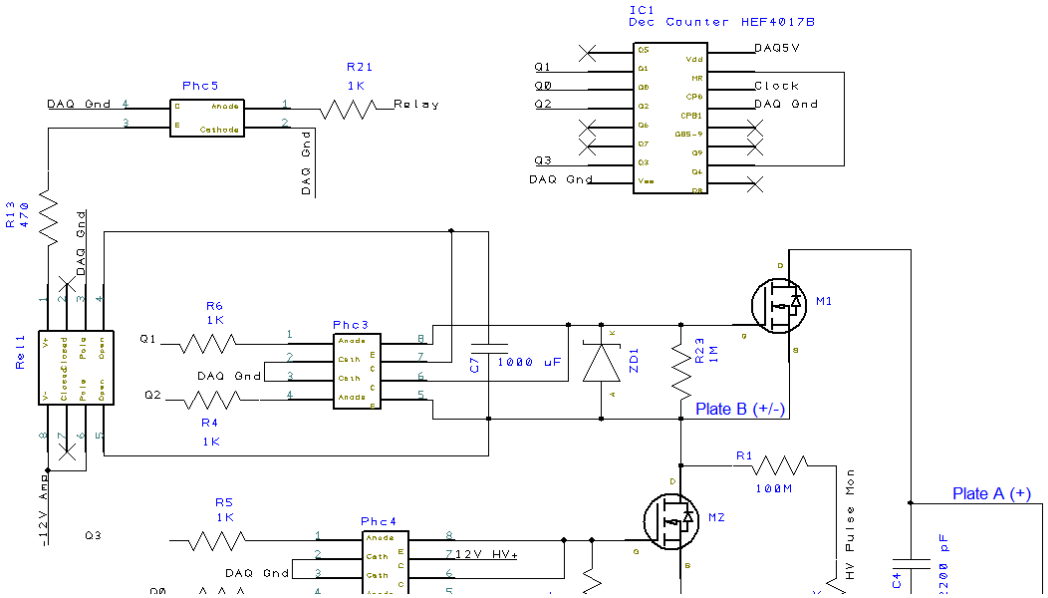

Fig 28 Circuit mediating generation of state-switching e-field. Zoom for detail. Schematic is continued in figures 29 and 30.

In one clock cycle, M1 charges the Plate B node to a high voltage (up to 2.4 KV). In another clock cyle, M2 discharges the Plate B node. Both M1 and M2 are NMOSFET. Ordinarily, M1 would be implemented with a PMOS transistor; however, a high voltage PMOS transistor was not

available. To isolate other parts of the circuit from high voltage, the gates of M1 and M2 are charged via photocouplers (photo-electric switches) designated Phc3 and Phc4 in figure 29.

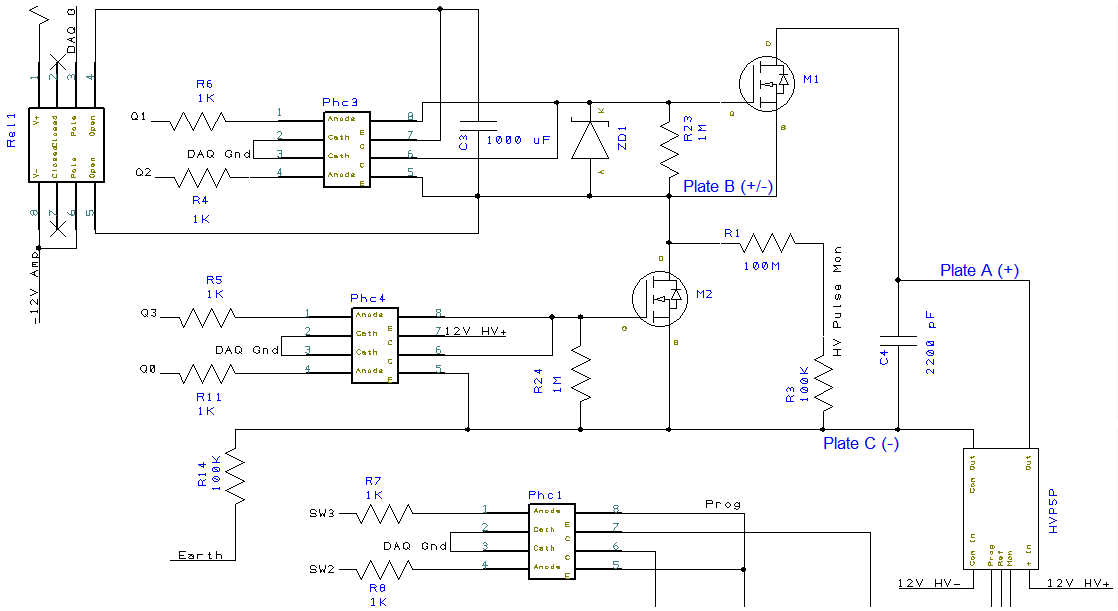

Fig 29 Circuit mediating generation of state-switching e-field. Zoom for detail. Schematic is a continuation of figure 28 above and culminates in figure 30 below.

As M1 is NMOS rather than PMOS, it is necessary to reference the Plate B node when applying a gate-source voltage. Since the Plate B node carries a high voltage, the power source for M1 requires isolation. This power source is implemented with a local capacitor (C3) in order to avoid loading the Plate B node with stray capacitance from wiring, which would severely reduce switching frequency. When C3 is depleted, it is recharged via a DPDT relay (Rel1) that connects C3 to a 12 [V] DC power source. The relay disconnects both leads of C3 from the DC supply when charging is complete in order to prevent loading the Plate B node with stray capacitance. Phc5 is a photocoupler that controls Rel1. Phc5 receives a digital signal from the DAQ device to activate or deactivate Rel1.

ZD1 is a zener diode connected to the gate and source of M1 and prevents damage to M1 from stray high voltage discharge. R23 and R24 keep M1 and M2, respectively, completely off when not activated by preventing buildup of trace gate-source voltages.

The switching photocouplers Phc3 and Phc4 each contain two separate photo-electric switches for a total of four switches. The decade counter, IC1 (figure 28), generates four digital signals (Q0-Q3) that control these switches, respectively. Only one switch in activated in a given cycle. For each transistor, one switch charges C_{gs} (the gate-source capacitance) and a second switch discharges it. With this switching mechanism, no overlap exists between the on-times of M1 and M2, thus avoiding a short-circuit current. R1 and R3 (figure 29) work as a voltage divider that provides an output that is one-thousandth the voltage at Plate B. This lower voltage makes it possible to monitor the high voltage on Plate B.

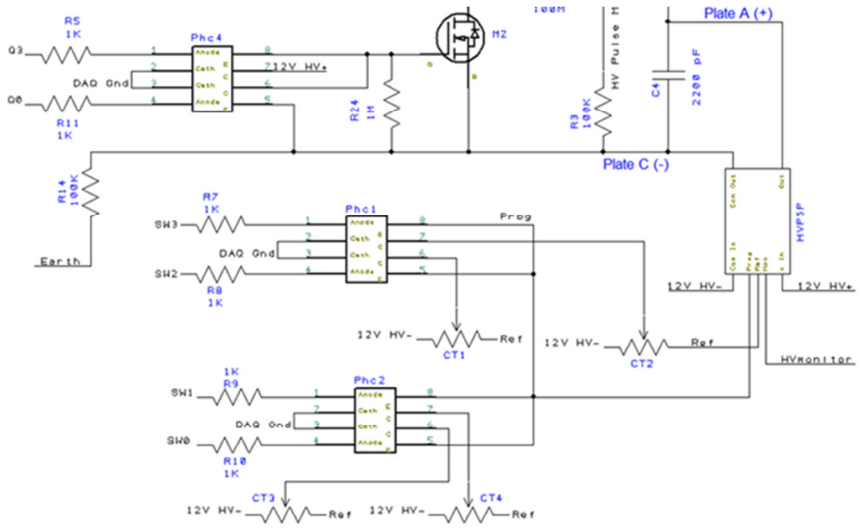

Fig 30 Circuit mediating generation of state-switching e-field. Zoom for detail. Schematic is a continuation of figures 28 and 29 above.

The component HVP5P (figure 30) is a high-voltage power supply and can deliver up to 1 [mA] of current. Its positive output connects to the Plate A node of the MMS (figure 13) and its negative output connects to the Plate C node of the MMS. The output voltage of HVP5P is

adjustable and is set in this circuit by one of four selectable potentiometers (CT1 – CT4). Phc1 and Phc2 are photocouplers that select which potentiometer is active. SW0-SW4 are digital select lines from the DAQ device that activate the corresponding photocoupler unit in Phc1 or Phc2. C4 stabilizes the output of HVP5P.

Figures 31 and 32 are schematics for the second division of the sensor circuit. This part of the circuit powers the ERVD pair and amplifies the output signal. In figure 31, the components labeled PL2 and PL3 respectively connect the two electrodes of the sample cell and the two electrodes of the reference cell to the circuit. Connected to both PL2 and PL3 are variable resistors (CT6 – CT9) for setting the value of R_L in both branches. Using two variable resistors in each branch allows for coarse and fine adjustment of R_L. Switches SW5a and SW5b disconnect the variable resistors from the circuit when their values are to be measured and set.

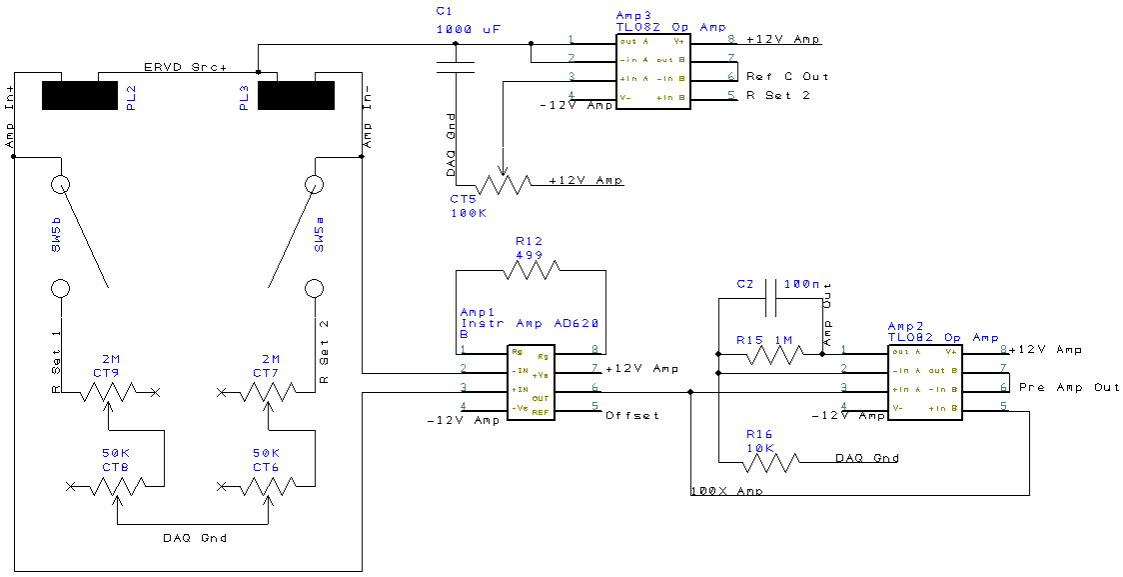

Fig 31 ERVD circuit with signal amplifiers, noise filter, and ERVD power source. Zoom for detail.

Amp1 is an instrumentation amplifier that amplifies the difference between the outputs of the ERVD pair by a factor of 100. The reference pin of Amp1 (pin 5) allows the output of the amplifier to be offset by a given voltage. This feature is put to use when it is necessary to "tare"

the output of the amplifier. Taring is performed when the signal from the ERVD pair exceeds the range of the amplifiers. Applying an offset voltage brings the signal back into range, provided that the signal does not exceed the available offset. Both the offset voltage and the amplifier output are recorded. During data analysis, the offset is subtracted from the modified sensor output in order to regain the true signal.

The Amp2 IC houses two separate op-amps, Amp2a and Amp2b. Amp2a amplifies the signal from Amp1 by another factor of 100 for a total gain of 10,000. R15 and R16 set the gain of Amp2a and C2 turns the amplifier into a low-pass filter to eliminate high frequency noise. Sources of noise include background RF and the state-switching electric field in the first division of the circuit. Amp2b is simply a voltage buffer for monitoring the output of Amp1 without degrading the signal.

Amp3, like Amp2, is actually two separate op-amps on one IC (Amp3a and Amp3b). Amp3a serves as a variable voltage source for the ERVD pair. Its output voltage is set by the potentiometer labeled CT5. Capacitor C1 suppresses noise that may otherwise arise in the op-amp output, thus creating a stable DC voltage supply. Amp3b is a voltage buffer for monitoring the output of the reference cell. Its input is connected to the node labeled "R Set 2," the output of the reference cell.

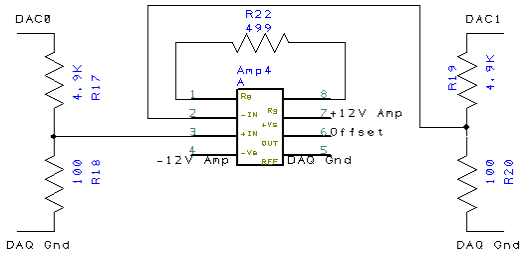

Fig 32 Circuit supplying offset voltage to Amp1. Zoom for detail.

Figure 32 is a schematic of the circuit that creates the offset voltage that is fed into Amp1 in figure 31. The nodes DAC0 and DAC1 are the outputs (with respect to ground) of two variable DC voltage sources in the DAQ device. One voltage source is fed into the positive input of Amp4

and the other is fed into its negative input. With this configuration, both positive and negative offset voltages can be created, depending on the settings of these voltage sources. R17 – R20 comprise voltage dividers that scale the DAC0 and DAC1 voltages down to manageable levels and also increase voltage-step resolution for finer control of the offset voltage.

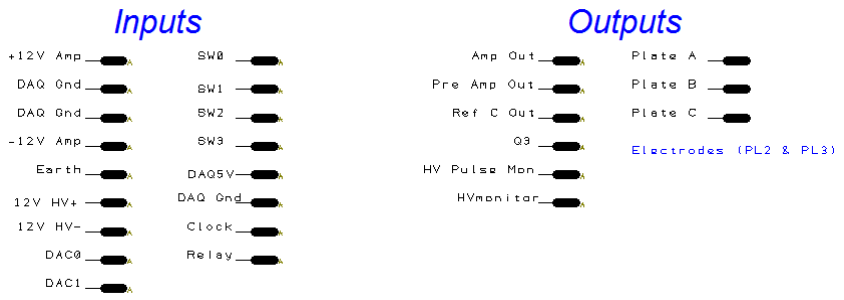

Fig 33 Summary of relevant inputs and outputs of the custom circuit. Zoom for detail.

Figure 33 organizes the most relevant inputs and output signals of the entire circuit. The first four inputs ("+12V Amp" through "-12V Amp") are pins for two DC power supplies for the amplifiers. The "Earth" pin grounds the high-voltage circuit that creates the two-state electric field. "12V HV+" and "12V HV-" are power-supply input pins for the high-voltage source, HVP5P. DAC0 and DAC1 are connections for software-controlled voltage sources on the DAQ device. They are referenced to the node "DAQ Gnd." SW0 – SW3 are digital signal lines from the DAQ device, only one of which is activated at a time; they control the output voltage of the high-voltage source, HVP5P, selecting from up to four pre-set voltages. "DAQ 5V" and "DAQ Gnd" are the supply rails from the DAQ devices. "DAQ 5V" delivers 5 [V] with respect to "DAQ Gnd." Clock is the digital frequency signal from the DAQ device and drives the state-switching of the electric field. The "Relay" digital signal turns relay Rel1 on or off.

For the outputs, "Amp Out" is the amplified, noise-filtered signal from the ERVD pair. "Pre Amp Out" outputs the signal from the first amplification stage for monitoring purposes. "Ref C Out" outputs the signal from the reference cell for monitoring. Q3 is for monitoring the state of the electric field. "HV Pulse Mon" outputs a scaled-down facsimile of the pulsed high-voltage that creates the state-switching electric field. This signal is for checking the proper operation of the

e-field generator circuit and is typically connected to an oscilloscope. “HVMonitor” allows monitoring of the high-voltage DC output of HV5P via a lower, more manageable voltage. Plates A-C connect to the MMS circuit board, which houses the sample and reference cells (figure 22). Electrode plugs PL2 and PL3 (shown in figure 31) also connect to the MMS circuit board, interfacing the electrodes in the MMS with the rest of the ERVD circuit on the main board.

APPENDIX C – Component Reference

Table 2 Lookup Reference for Specialized Components

Circuit Designation	Description	Manufacturer	Part Number/Name
IC1	Decade counter	NXP Semiconductors	HEF4017B
Phc1- Phc4	Photocoupler (switch)	Vishay Semiconductors	ILD1
Phc5	Photocoupler (switch)	Toshiba	TLP626
M1, M2	4KV NMOSFET	IXYS Corporation	IXTV03N400S
HVP5P	DC 5KV voltage source	Pico Electronics	HVP5P
Rel1	Mechanical relay	TE Connectivity	D3222
Amp1	Instrumentation amp	Analog Devices	AD620B
Amp4	Instrumentation amp	Analog Devices	AD620A
Amp2, Amp3	Op-amp	Radio Shack	TLO82

APPENDIX D – Software Code

Software that runs on a computer controls the DAQ. The DAQ may be programmed via this software. Below are the routines (code) that comprise the program for the current sensor implementation. The name of the routine or function appears above each printout. *Zoom to enlarge images.*

Table 3 Routine: initialize

```
/* This script is the first code to run when the DAQ
   software starts. It defines variables and constants that are
   used in other routines. Additionally, other initializations are
   performed here.
*/

using("device.labjack.")
include("c:\program files\labjack\drivers\labjackud.h")

global ID = 0  // DAQ device ID
global dac0    // Array to store measured DAC0 output values
global dac1    // Array to store measured DAC1 output values
global vArr = {0,600,1200,2400}     // Voltages to be output by high-voltage source
global hvLevel = 0 // High-voltage level index (0-3) for selecting output level

Define string dir = "C:\Path\Research\" + \
"ERVD Prototype\"

Define R15 = 1.004e6  // Measured value of Amp2a gain resistor #1
Define R16 = 1.006e4  // Measured value of Amp2a gain resistor #2
Define R17 = 4.87e3  // Measured value of R17 and R19 in circuit
Define R18 = 100     // Measured value of R18 and R20 in circuit
Define ampf = 100*(1 + R15/R16)  // Overall gain of Amp1 and Amp2A
Define divf = (R17+R18)/R18      // Voltage-divider factor for offset

/* Retrieve output values for DAC0 and DAC1 voltage sources for
   use in generating offset voltages in Amp1 */

private string fileName0 = dir + "DAC0.txt"  // File with measured values of DAC0 output
private string fileName1 = dir + "DAC1.txt"  // File with measured values of DAC1 output
private fhandle

try
   fhandle = file.Open(fileName0,1,0,0,1)
   dac0 = file.ReadDelim(fhandle,-1,",",chr(10),0)
   file.Close(fhandle)

   fhandle = file.Open(fileName1,1,0,0,1)
   dac1 = file.ReadDelim(fhandle,-1,",",chr(10),0)
   file.Close(fhandle)

catch()
   file.Close(fhandle)
   ? "File error in function initialize"
endcatch

// Initialize offset to zero by setting DAC0 and DAC1 sources to same value
posOutCh = 0.559
negOutCh = 0.559
```

Table 4 Routine: main

```
/* This is the main routine that calls all other routines (sub-routines),
   except the "initialize" routine. The "initialize" routine starts
   automatically when the software loads and executes once */

/* Determine file name for data file based on user selection.
   Variable "dir" is predefined in the "initialize" auto-start routine. */
private string fname = dir + \
"ERVD " + component.fileButton.strCaption + ".csv"

private j             // Loop counter
private dataPoints       // Data array
private fcount = 50      // Number of frequency points to probe
private preFreq       // Stores sensor output value before perturbation
private postFreq      // Stores sensor output value during perturbation
private clockFreq

// Create array to manage data from sensor before writing to file
// Also generate list of frequencies at which to perturb solutions
dataPoints = newDArray(fcount,vArr[hvLevel],100,100)

set_hv_level(0)   // Ensure that high-voltage source is off
setFState()       // Initialize e-field circuits to a known state
relayCh = 1     // Start charging supply capacitor C3
wait(1)         // Continue charging capacitor (allow 0.1 seconds to charge)
relayCh = 0       // End charging of C3
set_hv_level(hvLevel)   // Activate e-field (turn on high-voltage source)
wait(2)         // Allow HV source capacitor to charge
tare()          // Tare output

for(j=0, j<fcount, j++) // For each frequency
   setFState()       // Initialize e-field circuits to a known state
   wait(0.5)         // Allow analytes time to migrate to low-sensitivity electrode

   preFreq = readStable()  // Store sensor output before perturbation

   // Switch e-field state at calculated frequency and store actual circuit frequency
   if (dataPoints[j][2] == 0)    // If frequency is zero,
      freq_off()                 // turn off frequency output (don't switch e-field)
   else
      clockFreq = 4*dataPoints[j][2]
      clockFreq = freq_out(clockFreq)
      dataPoints[j][2] = round(clockFreq/4,1)
   endif

   postFreq = readStable()     // Store sensor output during perturbation

   dataPoints[j][0] = ampReadCh.Time[0]      // Save data acquisition time

   if(preFreq != -8888 && postFreq != -8888) // If the sensor output was stable,
      // record sensor output (subtract background signal first)
      dataPoints[j][3] = postFreq - preFreq
   else
      dataPoints[j][3] = -8888  // Sensor output was unstable; record error
   endif

   dataPoints[j][4] = round(refReadCh[0], 2)    // Save reference cell output

   freq_off()     // Turn off frequency output

endfor

saveData(fname,dataPoints,0)   // Write the data array to file

set_hv_level(0)      // Turn off e-field
```

Table 5 Sub-routine: freq_off()

```
// Turn off the clock signal that drives e-field state-switching
function freq_off()
   AddRequest(ID, LJ_ioPUT_CONFIG, LJ_chNUMBER_TIMERS_ENABLED, 0, 0, 0)
   GoOne(0)
   setStateCh = 0
```

Table 6 Function: freq_out()

```
// freq_out() outputs clock signal to drive e-field state-switching

function freq_out(frequency)

   // Get clock base and divisors
   private errMargin = 0
   private bd = null     // Array variable to hold clock base and divisors

   while(errMargin <= 30)
      try                // Get clock-base divisors for desired frequency, if possible
         bd = getbd(frequency, errMargin)
         break
      catch("NoFreq")
         errMargin+=2    // Increase error margin and try again
      endcatch
   endwhile

   if(isEmpty(bd))
      throw("NoFreq Error margin too small. Frequency: " + frequency)
   endif

   //Set the timer/counter pin offset to 8, which will put the first
   //timer/counter on E101.
   AddRequest (ID,  LJ_ioPUT_CONFIG, LJ_chTIMER_COUNTER_PIN_OFFSET, 8, 0, 0)

   // Use system clock
   AddRequest(ID, LJ_ioPUT_CONFIG, LJ_chTIMER_CLOCK_BASE, bd[0], 0, 0)

   //Set the divisor
   AddRequest(ID, LJ_ioPUT_CONFIG, LJ_chTIMER_CLOCK_DIVISOR, bd[1], 0, 0)

   //Enable 1 timer.
   AddRequest(ID, LJ_ioPUT_CONFIG, LJ_chNUMBER_TIMERS_ENABLED, 1, 0, 0)

   //Configure Timer0 as Frequency out.
   AddRequest(ID, LJ_ioPUT_TIMER_MODE, 0, LJ_tmFREQOUT, 0, 0)

   //Set the second divisor
   AddRequest(ID, LJ_ioPUT_TIMER_VALUE, 0, bd[2], 0, 0)

   //Execute the requests.
   GoOne(0)

   // Return actual frequency
   return bd[3]
```

Table 7 Function: getbd()

```
/* Determine clock base (1 MHz, 4 MHz, 12 MHz, or 48 MHz) to use to
   output frequency from DAQ device to custom circuit.
   Also calculate two divisors to divide the clock base to yield the
   desired frequency.
*/

function getbd(frequency, errMargin)  // Determine clock base & divisors

   private factor             // Product of divisors
   private result = {0,0,0,0} // Array to hold results
   private loopcnt1           // Counter for looping through base array
   private loopcnt2           // Counter for looping through divisors
   private error     // Difference between calculated and target frequency
   private testFreq  // Calculated frequency to be checked for error
   private base = {{23,1e6}, {24,4e6}, {25, 12e6}, {26,48e6}} // clock base
```

Table 7 continued

```
for(loopcnt1 = 3, loopcnt1 >= 0, loopcnt1--)

   result[0] = base[loopcnt1][0]    // Save code for specifying base

   factor = base[loopcnt1][1]/2/frequency // Calculate factor

   for(loopcnt2 = ceil(factor/256), loopcnt2 <= 256, loopcnt2++)

      result[1] = ceil(factor/loopcnt2)   // Save first potential divisor
      result[2] = loopcnt2                // Save 2nd potential divisor

      testFreq = base[loopcnt1][1]/(2 * result[1] * result[2])
      error = abs(frequency - testFreq)

      if(error <= errMargin)

         result[3] = testFreq     // Save actual frequency

         if(result[1] == 256)
            result[1] = 0         // 0 actually represents 256
         endif

         if(result[2] == 256)
            result[2] = 0         // 0 actually represents 256
         endif

         return result
      endif

   endfor
endfor


throw("NoFreq No divisors for input frequency")
```

Table 8 Function: newDArray()

```
/*
newDArray() creates an array for managing sensor data before
the data is written to file. Each row of the array has five fields
as listed below. The "e-field voltage" and frequency fields are pre-populated.
Other fields are the data to be acquired via the DAQ device.

Row fields (columns)
0: Data point aquisition time
1: E-field voltage (output of high-voltage source)
2: Frequency of state-switching e-field
3: Sensor differential output signal
4: Reference cell output signal
*/

function newDArray(size,voltage,freq1,freqIncr)

   private arr          // Variable to hold array
   arr[size-1][4] = 0   // Create array that has "size" # of rows and 5 fields (0-4)

   private i
   for(i = 0, i < size, i++)
      arr[i][1] = voltage     // Same voltage for all data points in a spectrum
      arr[i][2] = freq1 + i*freqIncr   // Generate frequency list with uniform interval
   endfor

   return arr
```

Table 9 Function: readPoint()

```
/* readPoint() samples the sensor output and subtracts the applied
   offset in order to reconstruct the signal */

 function readPoint()
    private diffIn
    private offset

    if(abs(ampReadCh[0]) > 9)  // If necessary,
       tare()   // apply offset voltage to strong sensor signal to avoid output clipping
    endif

    // Obtain amplified output of ERVD pair and divide by amplfication factor (gain)
    // in order to restore signal
    diffIn = round(ampReadCh[0],2)/ampf

    // Calculate offset voltage that was applied
    offset = (posOutCh[0] - negOutCh[0])/divf

    // Remove offset from signal and return value
    return round(diffIn - offset,6)
```

Table 10 Function: readStable()

```
/* Sample the sensor output after it stabilizes.
   Return error value if output signal does not stablize
   within alloted time. */

 function readStable()
    private previous     // Variable to store previous data point
    private present = readPoint() // Variable to store current data point
    private data = {0,0,0}  // Array for reading series of points to determine stability
    private count = 0       // Number of stable points that have been read
    private waitTime = 0.04    // Time to wait before attempting another read (seconds)
    private elapsed = 0        // Elapsed time in seconds
    private maxDelta = 5e-6  // Maximum allowed difference between two stable points (volts)

    while(count < NumRows(data) && elapsed < 5)
       wait(waitTime)
       elapsed += waitTime

       previous = present
       present = readPoint()

       if(abs(present-previous) <= maxDelta)
          data[count] = present
          count++
       endif

    endwhile

    if(count == NumRows(data)) // If enough stable points were sampled,
       return round(mean(data), 5)   // return their average.
    else
       return -8888   // Otherwise return error code
    endif
```

Table 11 Sub-routine: saveData()

```
// Save data-array to file

function saveData(string fname,dArray,append)

   private fhandle

   try
      fhandle = file.Open(fname,0,1,append,1)

      file.WriteDelim(fhandle,dArray,",",chr(10))
      file.Close(fhandle)

   catch()
      file.Close(fhandle)
      ? "File error in function saveData"
   endcatch
```

Table 12 Sub-routine: set_hv_level()

```
/* Select one of 4 output values for the high voltage source
   by activating one of three digital lines on the DAQ device.
   If none of the digital lines are activated, then the output
   voltage will be zero.
   (Up to four digital lines and voltage values can be set in
   the CC hardware. However, only three are implemented in software.)
*/

function set_hv_level(level)
   switch
      case (level==1)
         hvLevel2Ch = 0     // Turn OFF this digital line (channel)
         hvLevel3Ch = 0     // Turn OFF this channel
         hvLevel1Ch = 1     // Turn ON this channel
      case (level==2)
         hvLevel1Ch = 0
         hvLevel3Ch = 0
         hvLevel2Ch = 1
      case (level==3)
         hvLevel1Ch = 0
         hvLevel2Ch = 0
         hvLevel3Ch = 1
      default
         hvLevel1Ch = 0
         hvLevel2Ch = 0
         hvLevel3Ch = 0
   endcase
```

Table 13 Sub-routine: setFState()

```
/* Initialize electric-field control circuit so that e-field always
   initializes in a particular state, thereby always starting oscillation
   of analytes at the low-sensitivity electrode */

function setFState()
   private i

   for(i = 1, i <= 16, i++)
      read(getStateCh)     // Check the state by testing the Q3 output

      if(getStateCh[0])    // If the state is set (Q3 = 1)
         return
      endif

      // State not set, so output clock pulse and check again
      setStateCh = 0
      setStateCh = 1

   endfor

   // Generate error if state could not be set after multiple tries
   throw("setFState Could not initialize e-field circuit")
```

Table 14 Sub-routine: tare()

```
/* Tare sensor output signal if the input is so large as to result
   in clipping. Use digital-to-analog voltage sources DAC0 and DAC1
   to apply offset voltages to reverse the clipping, if possible.
   Increasing DAC0 INCREASES sensor output. Increasing DAC1 DECREASES
   sensor output. */

function tare()

   private count = 0     // Loop counter
   private preAmp        // Variable to store Amp1 output
   static index0 = 26    // Array index for tracking DAC0 output voltage
   static index1 = 26    // Array index for tracking DAC1 output voltage

   while(count < 500)    // Try up to 500 times
      preAmp = round(mean(preAmpCh[0,4]),2)

      if(abs(preAmp) < 0.04)  // If there's no clipping, exit
         return
      endif

      // There's clipping, so apply offset with either DAC0 or DAC1
      switch

         // Apply negative offset with DAC0
         case(preAmp > 0.02 && index0 > 0)
            index0--
            posOutCh = dac0[index0]

         // DAC0 at minimum, so use DAC1 to apply negative offset
         case(preAmp > 0.02 && index1 < 248)
            index1++
            negOutCh = dac1[index1]

         // Apply positive offset with DAC0
         case(preAmp < -0.02 && index0 < 248)
            index0++
            posOutCh = dac0[index0]

         // DAC0 at maximum, so use DAC1 to apply positive offset
         case(preAmp < -0.02 && index1 > 0)
            index1--
            negOutCh = dac1[index1]

         default  // Both DAC0 and DAC1 are maxed out, so do nothing
            break
      endcase

      count++
      wait(0.04)
   endwhile
```

APPENDIX E – Cell Configuration

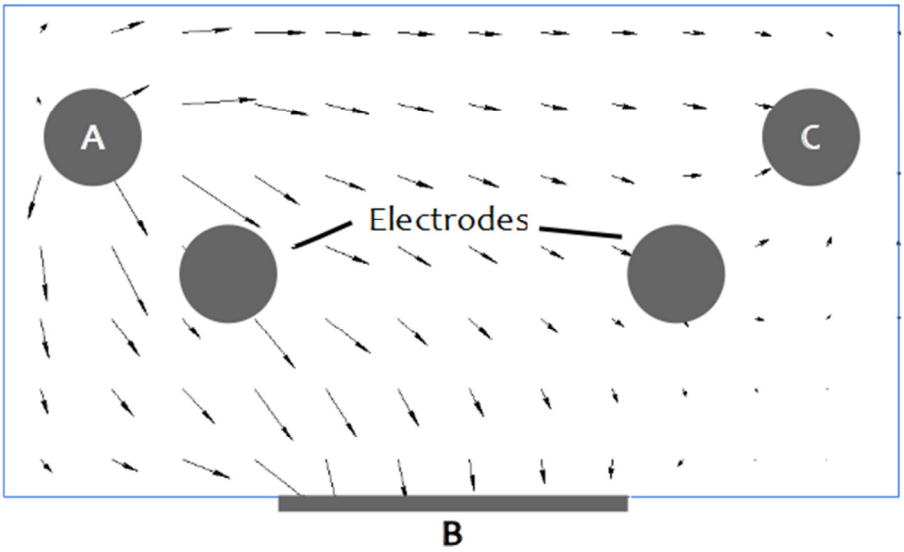

Fig 34 Simulation of the first state of the electric field, including the electrodes. The effects of the solution and the small potential applied to the electrodes by V_{src} are not included in the simulation. The simulation was performed with QuickField™ electrostatics software.

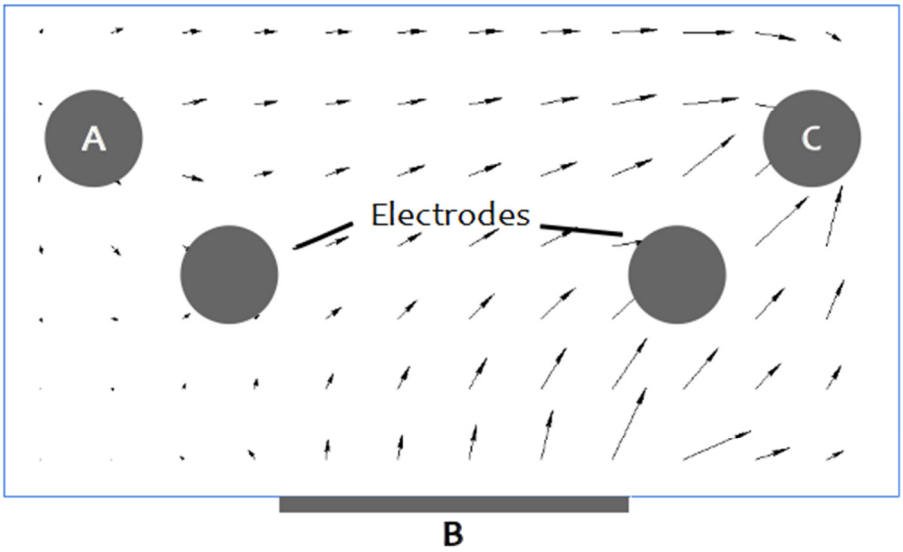

Fig 35 Simulation of the second state of the electric field, including the electrodes. The effects of the solution and the small potential applied to the electrodes by V_{src} are not included in the simulation. The simulation was performed with QuickField™ electrostatics software.

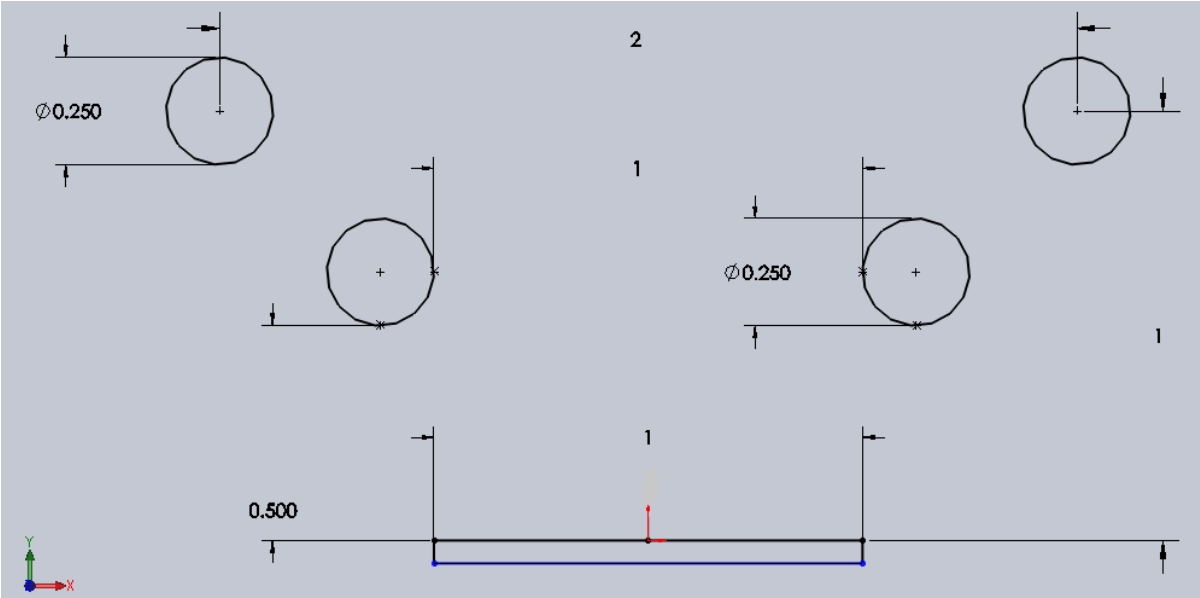

Fig 36 Electrode and plate dimensions in millimeters [mm].